INVESTIGATING SEISMIC AND ENERGY RETROFITTING BY IMPLEMENTING INNOVATIVE MATERIALS AND TECHNIQUES FOR MASONRY BUILDINGS

HAMZA TAHAT

JULY 2022

DİYARBAKIR

GRADUATE SCHOOL
OF NATURAL AND APPLIED SCIENCES
OF DICLE UNIVERSITY

INVESTIGATING SEISMIC AND ENERGY RETROFITTING BY IMPLEMENTING INNOVATIVE MATERIALS AND TECHNIQUES FOR MASONRY BUILDINGS

BY
HAMZA TAHAT

IN PARTIAL FULFILLMENT OF THE REQUIREMENTS
FOR
THE DEGREE OF MASTER OF SCIENCE
IN
CIVIL ENGINEERING

July 2022
DİYARBAKIR

INVESTIGATING SEISMIC AND ENERGY RETROFITTING BY IMPLEMENTING INNOVATIVE MATERIALS AND TECHNIQUES FOR MASONRY BUILDINGS

This study, prepared by **HAMZA TAHAT** as part of the Dicle University Graduate Education and Examination Regulation, was evaluated by the jury members with the following information and accepted as a **Master's Thesis in the Department of Civil Engineering**.

Prof. Dr. Neslihan DALKILIÇ
Dean, Graduate School of **Natural and Applied Science**

Assoc.Prof. Dr. İdris BEDİRHANOĞLU
Supervisor, **Civil Engineering Dept., Dicle University**

Examining Committee Members:

Assoc. Prof. Dr. Hasan ÖZKAYNAK (*)
Civil Engineering Dept., Beykent Üniversitesi

Assoc. Prof. Dr. İdris BEDİRHANOĞLU (**)
Civil Engineering Dept., Dicle University

Assoc. Prof. Dr. Mehmet Emin ÖNCÜ
Civil Engineering Dept., Dicle University

APPROVAL

Date: *30/07/2022*

(*) Write the title, name, and affiliation of the head of the examining committee in the first row.
(**) Write the title, name, and affiliation of the supervisor in the second row.

I hereby declare that all information in this document has been obtained and presented following the Thesis Manual (prepared by the Dicle University Graduate School of Natural and Applied Sciences), academic rules, and ethical conduct. I also declare that, as required by these rules and conduct, I have fully cited and referenced all material and results that are not original to this work. I shall be solely responsible if any evidence is found against my declaration.

Name, Surname: HAMZA TAHAT

Signature: ……………………………

ACKNOWLEDGMENTS

I would like to acknowledge the following people whose enormous contributions led to the successful completion of this thesis:

I would like to express my gratitude to my supervisor, "Associate Prof. Dr. IDRIS BEDIRHANOGLU" for providing me with this opportunity and for all of his support, encouragement, and guidance during my master's journey. I appreciate you sharing your passion, motivation and enthusiasm.

All my gratitude and love are for my family in Jordan, my parents ABDULSALAM and ARWA, grandfather, grandmother, my brothers and sisters for their invaluable support despite the distance and for encouraging me to be better and pursue my dreams.

Finally, I would like to express my gratitude to Dicle University, Department of Civil Engineering, for the facilities that they provided to me.

CONTENT

LIST OF FIGURES

LIST OF TABLE

ANNOTATION AND SYMBOL

Symbol	**Explanation**
A_f	The cross-section area of textile in TRM
l	Distance between supports
t_m	Masonry cross-section depth
t_c	Thickness of TRM composite
c	The neutral axis depth
z	Distance from extreme compression fibre to neutral
ε_m	Masonry strain in the compressed edge
ε_{m1}	Strain associated with the end of the parabolic shape
ε_{mu}	Masonry maximum compressive strain
ε_{fu}	The ultimate tensile strain of TRM
ε_{ffe}	Effective tensile strain in TRM
E_f	Modulus of elasticity of TRM
f'_m	Compressive strength of masonry

Annotation	**Explanation**
ACI 2013	American Concrete Institute
EC6	European Seismic Code

ABSTRACT

INVESTIGATING SEISMIC AND ENERGY RETROFITTING BY IMPLEMENTING INNOVATIVE MATERIALS AND TECHNIQUES FOR MASONRY BUILDINGS

HAMZA TAHAT

Master of Science in the Department of Civil engineering

Supervisor: Associate Prof. Dr Idris BEDIRHANOGLU

July 2022,80 pages

Unreinforced masonry buildings bear traces of previous civilisations' cultural and architectural monuments. They are considered a significant danger to humans because they have been proven to fail when exposed to earthquakes. In addition, there is a rising necessity to reduce our carbon footprint and thermal energy consumption. So, the behaviour of masonry walls retrofitted with textile-reinforced mortar (TRM) and thermal insulation to combine seismic and energy retrofitting has been investigated.

For this purposes, analytical work has been implemented using two equations developed by authors in the literature to estimate the out-of-plane maximum resisting bending moment of retrofitted masonry walls. The accuracy of the adopted equations has been evaluated by comparison of the results of equations with corresponding experimental results from a database comprising 108 TRM-strengthened walls collected from the literature.

In addition, the development of finite element (FE) model has been investigated for seismic and energy retrofitting of masonry walls through the application of the TRM systems and thermal insulation panel (TIP).

In addition, the development of a numerical method has been investigated through the application of the TRM systems and thermal insulation panel (TIP) for seismic and energy retrofitting for masonry walls by the finite element (FE) method. Five parameters have been investigated through FE analysis: unreinforced masonry wall as control specimen; only TRM composite has been bonded to both sides of the wall without TIP; both TRM and TIP have been bonded to both sides of the wall; only TIP has been implemented to both sides of the wall without TRM systems; both of TRM and TIP have been applied to only one side of the wall.

The analytical results indicate that the equation developed in the literature to predict the capacity of FRP-retrofitted URM walls provides acceptable results to predict the capacity of TRM-retrofitted URM walls. The results of the FE method agree with the results of the previous studies.

Keywords: Masonry buildings, Seismic retrofitting, Energy retrofitting, Textile-reinforced mortar (TRM), Flexural capacity, Thermal insulation panel, Finite element analysis.

ÖZET

YIĞMA YAPILAR İÇİN YENİLİKÇİ MALZEME VE TEKNİKLER KULLANARAK YIĞMA YAPILARIN SİSMİK VE ENERJİ GÜÇLENDİRMESİNİN ARAŞTIRILMASI

HAMZA TAHAT
Yüksek Lisans, İnşaat Mühendisliği
Danışman: Doç. Dr İdris BEDIRHANOĞLU
Temmuz 2022, 80 sayfa

Yığma yapılar, eski uygarlıkların kültürel ve mimari eserlerinin izlerini taşımaktadır. Bazı yığma yapılar insanlar için önemli bir tehlike olarak kabul edilirler çünkü depremlere maruz kaldıklarında. Yıkıldıkları görülmektedir ve dolayısı ile bir çok yığma yapının deprem performanslarının iyileştirilmesi gerekmektedir. Diğer yandan, karbon ayak izimizi ve termal enerji tüketimimizi azaltmak için artan bir ihtiyaç olmasından dolayı bu yapıların enerji tüketimim açısından da performanslarının iyileştirilmesi gereklidir. Bu nedenle bu çalışmada, sismik ve enerji güçlendirmeyi birleştirmek için tekstil takviyeli harç (TRM) ve ısı yalıtımı ile güçlendirilen yığma duvarların davranışı araştırılmıştır.

Bu amaçla, literatürde mevcut araştırmacılar tarafından geliştirilmiş iki denklem kullanılarak, güçlendirilmiş duvarlarının düzlem dışı eğilme kapasitelerini tahmin etmek için analitik çalışma gerçekleştirilmiştir. Kabul edilen denklemlerin doğruluğu, literatürden toplanan 108 TRM ile güçlendirilmiş duvardan oluşan bir veri tabanından ilgili deneysel sonuçlarla denklem sonuçlarının karşılaştırılmasıyla değerlendirilmiştir.

Ayrıca, TRM sistemleri ve ısı yalıtım paneli (TIP) uygulamasıyla yığma duvarların sismik ve enerji güçlendirmesi için sonlu elemanlar (FE) modelinin geliştirilmesi araştırılmıştır.

Sonlu elemanlar yöntemi ile yığma duvarlar için sismik ve enerji güçlendirmesi için TRM ve ısı (TIP) beraber uygulanarak sayısal bir yöntemin geliştirilmesi araştırılmıştır. FE analizi yoluyla beş parametre araştırılmıştır: kontrol numunesi olarak donatısız duvar; TIP olmadan duvarın her iki tarafına sadece TRM kompozit yapıştırılmıştır; hem TRM hem de TIP duvarın her iki tarafına yapıştırılmıştır; TRM olmadan duvarın her iki tarafına sadece TIP uygulanmıştır; hem TRM hem de TIP duvarın sadece bir tarafına uygulanmıştır.

Analitik sonuçlar, literatürde FRP ile güçlendirilmiş unreinforced masonry (URM) duvarlarının kapasitesini tahmin etmek için geliştirilen denklemin, TRM ile güçlendirilmiş URM duvarlarının kapasitesini tahmin etmek için kabul edilebilir sonuçlar sağladığını göstermektedir. FE yönteminin sonuçları, daha önceyapılan çalışmaların sonuçlarıyla uyumludur.

Anahtar Kelimeler: Yığma binalar, Sismik güçlendirme, Enerji güçlendirme, Tekstil takviyeli harç, (TRM), Eğilme kapasitesi, Isı yalıtım paneli, Sonlu elemanlar analizi.

1. INTRODUCTION

1.1 Background and Motivation

Unreinforced masonry (URM) buildings are structures built by stacking construction materials like bricks and stones without reinforcing materials or using minimum reinforcement needs of less than 25% (FEMA, 306.1998). URM buildings are the world's oldest building types. They are a significant risk to humans because they fail when exposed to earthquakes or wind pressure. Moreover, cumulative damage from earthquakes or structural collapse resulting from ageing is considered a direct threat to the keeping and protection of masonry buildings, which contain substantial components of numerous countries' cultural heritage. Therefore, there is a pressing necessity to retrofit current masonry structures in seismic regions where buildings built using old seismic design standards must meet the higher performance levels required by current seismic design codes, and in non-seismic places, due to a change in usage or the introduction of stricter engineering standards(Triantafillou et al., 2017).

In developing countries, masonry structures as homes designed by their owners without returning to engineering principles. Local workers implement them without following engineering code recommendations due to their low cost and ease of construction. Even in developed countries, URM structures were found decades ago without engineering principles. They have been built in seismically prone zones where the philosophy of seismic design was at the beginning. Therefore, most URM structures do not meet seismic design standards. Many URM buildings have suffered collapse and destruction due to medium and robust earthquakes, causing extensive property and livelihood losses. As a result, over the past two decades, many tests have been performed on URM buildings to develop seismic performance, and the results have been promising (Bothara et al., 2010). The reason for the lack of understanding of URM's building behaviour is the diversity of its construction, non-engineering principles, and non-standard design (Bothara and Hiçyılmaz, 2008). The age of the buildings and regional differences in the building materials and techniques used were also affected (Bothara et al., 2010).

The failure mechanisms of URM are out-of-plane and in-plane mechanisms. The first mechanism only influences parts of the wall. It occurs when a wall is exposed to an out-of-plane loading, and there is an inadequate anchorage of the perpendicular walls or an inadequate connection between the floor and walls. The second mechanism influences entire panels and occurs when a load is exerted in the same plane of the masonry wall. Figure 1.1 shows both the failure mechanisms of masonry (Bucchi et al., 2013).

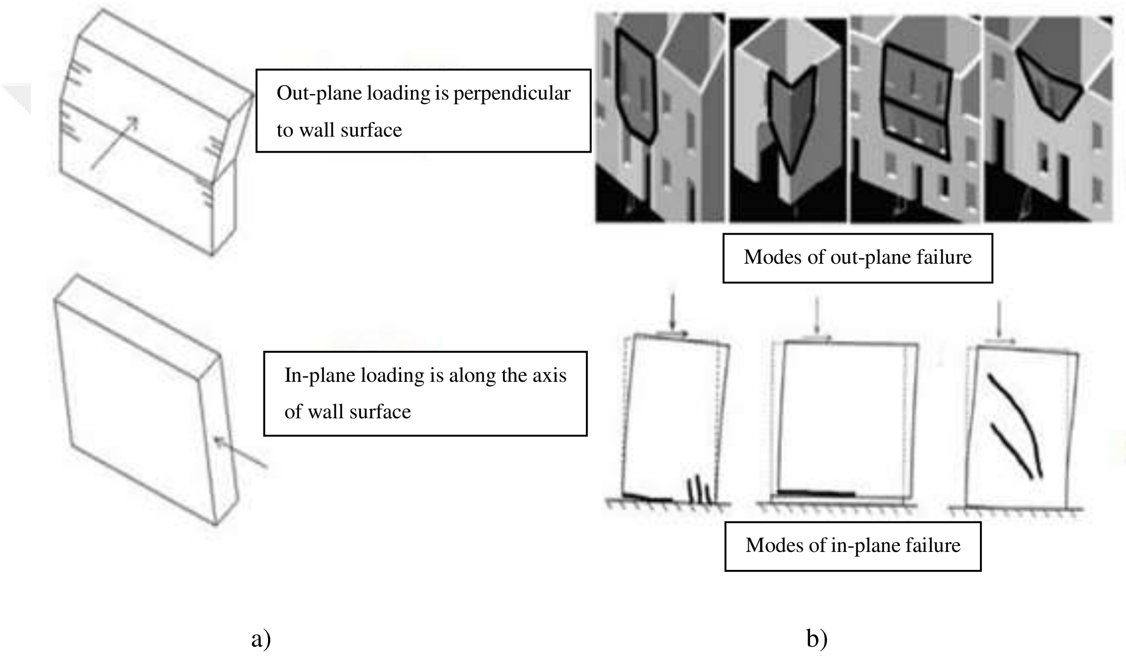

Figure 1.1 Types of masonry failure a) Out-of-plane and in-plane behaviour of a single wall and b) modes of mechanisms (Bucchi et al., 2013)

The structural performance of masonry walls under in-plane loading is better than that of out-of-plane, Due to their in-plane stiffness. URM walls exhibit flexible behaviour and respond poorly in perpendicular directions to seismic movement. Therefore, shear forces become active in-plane of the wall, leading to an in-plane mode. Because a flexural mechanism develops in the weak direction, an out-of-plane mechanism is developed. This study is interested in retrofitting URM walls under out-of-plane loading. Figures 1.2 and 1.3 display collapsed masonry buildings.

Figure 1.2 Total damage to the masonry house (Taken from the archive of Assoc. Prof. Dr. İdris Bedirhanoğlu, Bedirhanoglu 2011a)

Figure 1.3 Diagonal damage to the masonry house after the Van Earthquake 2011 (Taken from the archive of Assoc. Prof. Dr. İdris Bedirhanoğlu, Bedirhanoglu 2011a)

At the same time, because of the increasing awareness of the environmental influence of the structures around us, they are greatly affected by the existing building inventory because of energy consumption and CO_2 emissions. The sector expands about 36% of the world's energy and releases 39% of overall carbon dioxide (Benzar et al., 2020). The reasons for the unsatisfactory energy behaviour of older buildings are the absence or obsolescence of energy behaviour guidelines, seismic design rules at a stage of their construction, and the degradation and ageing of construction materials (Pohoryles et al., 2020). For that reason, the department of sustainable energy has become part of the conservation strategy for heritage and historical constructions and part of modern buildings' design, improving thermal energy efficiency (De Santoli et al., 2014).

However, if each retrofitting is applied separately, the result may be unsatisfactory since significant seismic risks might influence the existing building's environmental affecting. If the buildings are located in an earthquake zone, the upgraded buildings, in terms of energy modification, will always be affected by structural damage. Thus, when an earthquake occurs, structures will suffer failures that may lead to breakdown based on severity, resulting in a threat to the population and turning thermal modernisation into a practical waste of funds. Structures that are only seismically modified will be effective in seismic performance because buildings will consistently spend much energy trying to compensate for the inherent heat losses caused by outdated construction activities (Belleri and Marini, 2015). Based on the above, it is necessary to research solutions to combine retrofitting seismic and energy using innovative materials and techniques.

The best way to conquer the challenges above is not to find a separate solution to each problem but to find an integrated solution to both problems so that both problems should be applied at the same time until we end up with an earthquake-proof and energy-resistant building. This integrated approach requires an initial investment but is often unavailable in many cases. However, when considering the lower combined retrofitting costs than separated retrofitting, it is the more reasonable choice to follow because of labour and scaffolding costs and the economic advantages of combining retrofitting simultaneously. For that, it is highly recommended that engineers improve innovative technologies and materials (Gkournelos et al.,2019).

Figure 1.4 shows energy against combined energy and seismic upgrading.

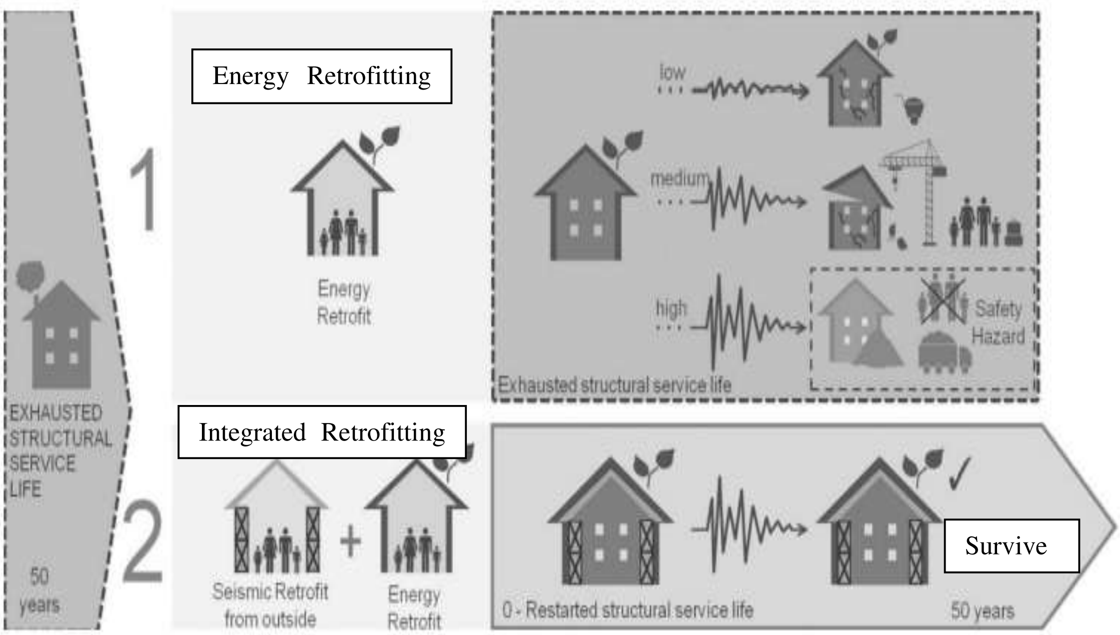

Figure 1.4 Energy versus integrated energy and seismic retrofitting (Gkournelos et al., 2019)

Multiple techniques are used to increase the strength and/or deformation capacity of masonry walls, such as the application of metallic or polymer-based grid-reinforced surface coatings, internal or external prestressing with steel ties, shotcrete overlays, externally bonded or near-surface mounted fibre-reinforced polymers (FRP) as well as textile reinforced mortar (TRM) techniques. External FRP techniques are more commonly used for retrofitting reinforced concrete (RC) because they resist shear forces for RC frame structures (Bedirhanoglu et al., 2022). Regarding the retrofitting of RC structures, there are different studies (Bedirhanoglu et al., 2013) implemented high-performance fibre-reinforced cementitious composite (HPFRCC) system to retrofit a deficient reinforced concrete exterior beam-column joints constructed with low-strength concrete. Also, (Bedirhanoglu, 2015) developed prefabricated-HSPRCC panels using high-performance concrete and perforated steel plate for retrofitting reinforced concrete members. Prefabricated-HSPRCC combines the benefits of steel and high-performance concrete. In addition , the FRP systems were tested to reinforce the shear strength and ductility of the short columns by (Bedirhanoglu et al., 2019). Types of fibre-reinforced cementitious composites for retrofitting reinforced concrete structures and applications described by (Bedirhanoglu and Ilki, 2018).

Regarding solutions based on TRM systems for masonry buildings, they are becoming more and more promising since they combine the advantageous characteristics of FRP systems regarding high strength and stiffness-to-weight ratio, high deformation capacity, corrosion resistance, speed and ease of enforcement, and little change in the geometry.

In addition to that, TRM jackets solve the majority of the challenges resulting from the utilisation of organic resins, such as poor performance at high temperatures, incompatibility with substrates, combustibility, high costs of epoxies, lack of breathability, difficulty in conducting post-earthquake assessment behind FRP jackets, reversibility requirements, and possible risks for the workers (Triantafillou et al., 2016). The TRM composite, also called textile-reinforced concrete (TRC) or fabric-reinforced cementitious matrix (FRCM), consists of an open-weaved fabric made of long woven, knitted or even unwoven fibre rovings in at least two (typically orthogonal) directions and an inorganic mortar matrix (Triantafillou et al., 2006). The density, defined as the quantity of the spacing of rovings in each direction, may be controlled independently, consequently affecting the mechanical characteristics of the open-weaved fabric and the degree of penetration of the mortar matrix through the woven mesh (Triantafillou et al., 2016).

Fibre dates back to ancient Egyptian times when organic fibre was employed to strengthen clay. Many organic and inorganic fibres are spread and vary in size, shape, and characteristics according to the material made of them (i.e. glass, cellulose, steel, micro-synthetic, macro-synthetic, natural, and poly-vinyl alcohol fibres) (Bedirhanoglu and Ilki, 2018). The fibres have different implementations according to their characteristics. The most common fibres used today are; carbon, glass, steel, basalt, and polypropylene (PP), as in Figures 1.5 and 1.6.

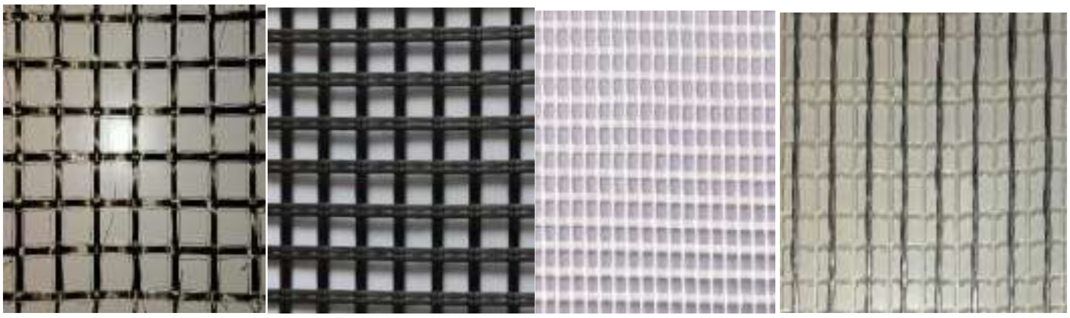

a) Basalt b) Carbon c) Glass d) Steel

Figure 1.5 Fibres in textile form (Majumder et al., 2021)

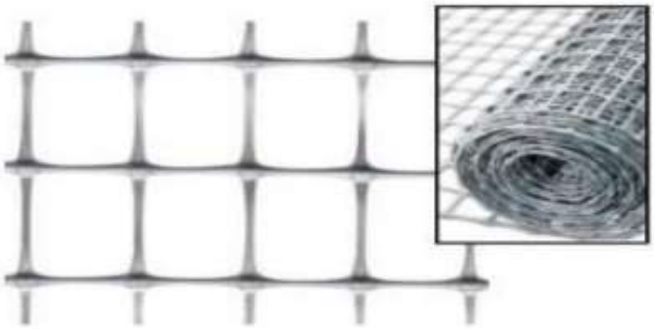

Figure 1.6 Polypropylene net (Mustafaraj et al., 2020)

The cement-based matrix and lime mortar matrices are the most common matrix used in TRM systems. (Mechtcherine et al., 2016). TRM techniques were utilised to increase the strength of tuff masonry walls investigated in diagonal compression by (Faella et al., 2004) (Prota et al., 2006), as well as in the form of confining jackets for small-scale rectangular column-type masonry samples examined in uniaxial compression by (Krevaikas**,** 2005) (Nurchi and Valdes, 2005), also for seismic retrofitting of URM walls exposed to in-plane or out-of-plane loading via (Papanicolaou et al., 2007) (Papanicolaou et al., 2008). In addition to other investigations concentrated on bond testing and behaviour by (D'Ambrisi et al., 2013) (De Felice et al., 2014) (Alecci et al., 2016) (Askouni and Papanicolaou, 2016), in-plane loading of walls by (Parisi et al., 2011), out-of-plane loading of walls by (Harajli et al., 2010) (Babaeidarabad et al., 2014), while by (Garmendia et al., 2011) for strengthening of arches, and seismic modification of infill masonry walls by (Koutas et al., 2015) (Koutas et al., 2015). In the current study, TRM systems have been adopted for seismic retrofitting.

Despite experimental and analytical studies being performed to investigate the TRM mechanical and bond behaviour, analytical investigations to assess the TRM contribution to the retrofitted URM walls are limited in the literature. Furthermore, the Italian CNR-DT 215 and American ACI 549.4R-13 are the only currently existing guidelines for constructing and designing TRM retrofitting techniques (D'Antino et al., 2022). Therefore, one of the current research aims is to predict the TRM contribution in terms of flexural capacity for masonry walls after TRM application.

Many techniques have been developed for energy retrofitting, with external and internal insulations becoming increasingly common because of significant energy storage, quick and easy implementation, and low cost (Bomberg et al., 1997) (Anastaselos, et al., 2014). Different thermal insulation panels are presently applied in external and internal insulation, mainly manufactured using expanded polystyrene (sintered or extruded), expanded polyurethane, and mineral wool. Both TRM composites with thermal insulation panels have been implemented in the current research for integrated retrofitting of masonry walls because TRM composite has low if any, thermal insulation capacity. In contrast, external or internal insulation has no load-bearing capacity (Triantafillou et al., 2017). Figure 1.7 shows TRM with themal insulation panel for masonry wall retrofitting.

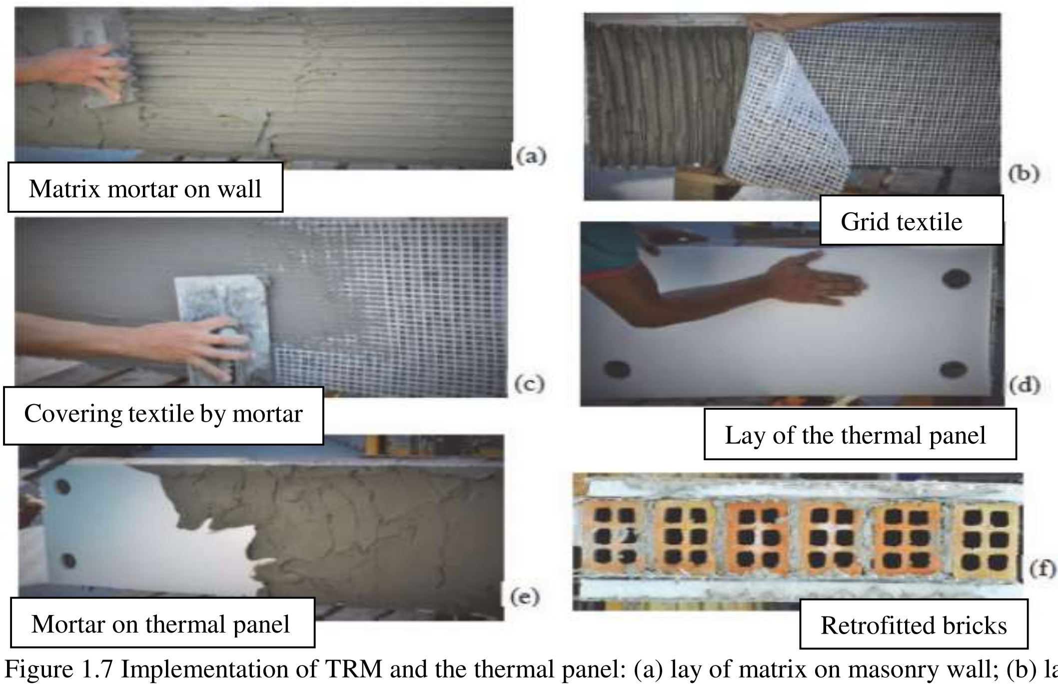

Figure 1.7 Implementation of TRM and the thermal panel: (a) lay of matrix on masonry wall; (b) lay of textile; (c) impregnation of textile with matrix; (d) lay of the thermal panel; (e) lay of mortar on top of the thermal panel; (f) typical cross-section of masonry wall (Triantafillou et al., 2017).

A numerical study is becoming a suitable substitute for experimental tests, using various numerical approaches such as the finite element (FE) method,discrete element method (DEM), and the applied element method (AEM) have been used to perform numerical investigation and simulate linear and non-linear behaviour of masonry (Abdulla et al., 2017). Therefore, the FE method has been used in the current thesis.

Finally, considering all those above, the primary vital issues in this study are the necessity to combine the seismic and thermal responses of URM buildings under out-of-plane loading using numerical investigation and the necessity to analytically predict the TRM contribution to the strengthened masonry walls under out-of-plane loading.

1.2 Scope and Objectives

The main aim of this thesis is to provide an analytical prediction of TRM's contribution to the seismic retrofitting of masonry walls and to comprehensively investigate the use of seismic and energy retrofitting of URM walls through the use of FE analysis. These aims will be achieved through the following enabling objectives:

a) To analytically assess the bearing capacity of TRM-reinforced masonry walls according to approaches available in the literature.
b) To develop an efficient FE modelling capable of predicting the behaviour of the seismic and energy retrofitting URM walls using TRM systems with thermal insulation materials and to investigate the effect of parameters on the performance of the walls.

The principal scope of this study is to analytically predict of capacity for TRM-retrofitted masonry walls undergoing out-of-plane loading, where energy retrofitting for masonry wall has been ignored.

Furthermore, the FE method to simulate the retrofitted URM wall by the TRM material and the thermal insulation panel (TIP). Masonry wall subjected to out-of-plane loading has been implemented in the ABAQUS software.

Finally, the research results are intended to compare the performance of mechanically studied models in the current study in predicting the capacities of TRM-reinforced URM walls and add essential data to the current literature about the combination of seismic and energy retrofitting by FE analysis.

1.3 Outlines

This work is divided into five chapters. The current study's motivation, scope, and objectives are outlined in the first chapter. The other chapters are arranged in the order shown below.

Chapter Two: Literature review

It presents the previous studies on two main topics. The first relates to analytical methods to predict maximum bending capacity for TRM-retrofitted masonry walls under out-plane loading—the second topic concerns using the TRM systems with thermal materials for seismic and energy retrofitting for URM walls.

Chapter Three: Analytical study

It presents the two methods to predict the capacity of TRM-retrofitted URM walls exposed to out-of-plane loading. It also presents a database of many tests of TRM-reinforced masonry walls. Finally, it presents the accuracy of the methods by comparing the results of the methods with the experimental results in the database.

Chapter Four: Finite element analysis of the retrofitted masonry wall

It gathers seismic and thermal retrofitting of masonry walls by various TRM systems with thermal insulation material using FE analysis in the ABAQUS software, as well as the results of the effectiveness of FE analysis by comparing the ABAQUS results with an experimental and numerical study in the literature.

Chapter Five: Results, Conclusion, and Future work

The last chapter of the thesis summarises all the chapters performed and synthesises the results reached in each of the chapters of the current thesis. Finally, it depicts proposed works and recommendations for future work.

2. LITERATURE REVIEW

This chapter summarises previous research on design methods for achieving maximum bending capacities of TRM-retrofitted masonry walls under out-of-plane loading, as well as combining seismic and thermal retrofitting of masonry walls using TRM systems with thermal insulation materials (TIM).

2.1 Prediction of flexural strength for TRM-strengthened masonry walls

Much research has been carried out to predict the flexural capacity of retrofitted URM walls. Mainly some studies related to TRM retrofitting have been summarised in the following.

Haraji et al., (2010) used a simple flexural model related to the type of failure. By consideration, compression force across the depth of the section should be concentrated at or near the tip of the block as monitored from the failure type of the samples. They applied a strain reduction factor to calculate the masonry shear failure and TRM debonding. The tested tension strain of the textile nets generated at flexural failure for the TRM-retrofitted specimens ranged from 20% to 70%, averaging 48% of the textile rupture strain.

Sagar et al., (2017) estimated the out-of-plane flexural strength of TRM-upgraded masonry walls by several available expressions from the literature. Then the expressions were compared with their corresponding experimental outcomes to determine a better expression. They adopted the expressions that were developed by Harajli et al., (2010), and ACI 549.4R (ACI 2013) for TRM-retrofitted masonry, as well as the equations created by Hamoush et al., (2001), Tan and Patoary, (2004), for FRP-retrofitted masonry. The experimental outcomes showed that the mean moment capacities of the reinforced samples for the failure plane orthogonal and parallel to the bed joint were 0.44 and 0.60 KN.m, respectively. The expressions outcomes showed a consistent assessment of flexural strength readings, ranging from 0.36 to 0.40 and 0.46 to 0.50 KN.m KN.m for the failure plane orthogonal and the parallel to the bed joint. Moreover, the expression developed by Tan and Patoary, (2004) showed more accurate assessment.

D'Antino et al., (2018) proposed that TRM system stress-strain behaviour be accounted for based on bond tests of masonry walls (single-or double-lap shear tests, bending tests, or pull-out tests). The results were compared with the ACI 549.4R-13 code and the suggested approach by Ascione et al. (2015) using a database containing sixty-three TRM-upgraded walls from previous experiments. It was concluded that their method provided accurate results. In contrast, the results of the ACI 549.4R-13 code and the approach created by Ascione et al., (2015) tended to underestimate the ultimate experimental moment, giving low accuracy.

Padalu al.,(2019) proposed a theoretical model using the ordinary beam theory by considering the strength of the masonry in tension, which contribution cannot be ignored in the bending strength estimation, particularly in the case of the debonding failure type. They demonstrated that the developed model evaluates the experimental moment capacity with a closely matching mean value (M_{exp}/M_{anal} = 1.04) and the least dispersion (COV = 0.21) compared with the available models. The developed model also determined the load-displacement curve quite closely to the one observed experimentally.

Meriggi et al., (2020) adopted the outcomes of TRM-to-substrate single-lap shear bond tests and clamping-grip direct tensile tests on bare textile samples, as proposed in recent guidelines. According to the comparison of analytical expressions with an experimental database that contains roughly 100 examinations, this work concluded that the ultimate tensile strain for the TRM systems has to be defined as the minimum between the bond strength amplified by a factor α_1 = 1.5 and the fabric tensile strength.

Tripathy al., (2020) evaluated ultimate flexural strength by investigating predictive formulations in the literature which were developed by Harajli et al., (2010); ACI 549.4R (ACI 2013); Padalu et al., (2019), and Meriggi et al., (2020) for TRM retrofitting and originally used equations for FRP systems by Triantafillou, (1998), Tumialan et al., (2003), Tan and Patoary, (2004), and Mosallam, (2007). For lime-based TRM, most of the used equations considerably underestimated the ultimate capacity, with analytical formulations of Harajli et al. (2010) and ACI 549.4R (ACI 2013) assessing very low capacity. This can be because of neglecting the effect of the bond in these theoretic formulations. The approach created by Triantafillou (1998) presented a more accurate assessment.

2.2 TRM systems with thermal materials for integrated retrofitting URM walls

There are limited studies on using TRM composites with thermal materials for integrated retrofitting URM walls. Particularly those studies are summarised in the following.

Triantafillou et al., (2017) studied combining TRM and thermal insulation panels for the structural and thermal improvement of building walls manufactured from clay bricks provided via a local factory and general-purpose cement-based mortar. The method was investigated on brick-building wallets that were periodically bended out-of-plane. Some wallets were tested for fire before mechanical investigations to estimate the efficiency of the method in actual fire circumstances. The method upgraded the thermal behaviour of masonry walls and was highly effective as a structural modernisation. Regarding fire-prone wall strength and deformation capacity, using both TRM with insulation was preferable to using TRM alone. The results displayed that the method provided the solution for combining seismic and energy retrofitting of the masonry wall subject to out-of-plane loading.

Triantafillou et al., (2018) introduced an innovative method for the structural and thermal upgrading of brick-building wallets through combined TRM for seismic upgrading and thermal insulation panels for energy retrofitting. The method was experimentally investigated by conducting medium-sized tests on three sets of clay brick construction walls subject to periodic in-plane loading. Each series of wallets consists of samples with retrofit systems, including using one-side instead of two-sides insulation and/or TRM, placing TRM outside the thermal panel or between the thermal panel and brick construction wall. The results displayed that the TRM could be efficiently blended with the thermal panel to significantly raise the capacity of samples exposed to periodic loading in-plane systems.

Karlos et al., (2020) studied combining the TRM and thermal materials for seismic and thermal modifications for masonry walls. Many medium-sized tests were performed on masonry walls that underwent periodic loading outside the plane. Different parameters have been tested; design of the textile-reinforced mortar in sandwich form; down and over insulation or outside insulation; single-side or two-sides TRM and/or insulation; displacement capacity of loading cycles. The outcomes gained from the study ensure that the TRM can be efficiently combined with insulation, growing the panels' overall strength and power behaviour. Also, They simulated the experimental tests for brick masonry walls using FE in the ANSYS program. Also, they reached that the FE method could reproduce the observed behaviour except for the post-peak reduction of strength because of constraints of the numerical approach to simulate stress-strain curves with negative slopes.

2.3 Conclusions

The first section of the literature review presents the analytical predictions of the capacity of reinforced masonry walls with TRM systems under out-of-plane loading using many equations developed by different researchers. Analytical results generally indicated that using the bond and tensile test results to obtain TRM stress-strain behaviour was more accurate. Few studies prove the usability of expressions proposed for FRP-retrofitted URM walls to predict the flexural strength of TRM-retrofitted URM walls.

Based on the above, in chapter three of the current study, two equations developed in the literature have been selected to predict the TRM contribution to the retrofitted URM walls. The first equation is proposed for TRM-retrofitted URM walls, while the second equation is submitted for FRP-retrofitted URM walls. Regarding TRM parameters, which have been used in both equations, the bond and tensile test results have been adopted to obtain the TRM stress-strain behaviour.

The second part of the literature review presents integrated seismic and energy retrofitting of masonry walls by combining the TRM systems and thermal insulation materials. All studies used TIP systems with TRM systems, and the results were efficient for integrated retrofitting. Nevertheless, the studies were very limited in the current literature. Also, only one study used FE approach to investigate the combining of the TRM system with the TIP system for masonry walls under out-of-plane loading. This study did not investigate the effects of the TIP system on masonry walls without the TRM system. As a result, this thesis uses FE analysis to perform more investigations into the effectiveness of combining TRM systems with the TIP systems for masonry walls under out-of-plane loading, as well as investigating the contributions of TIP in increasing the capacity of URM walls.

3. ANALYTICAL STUDY

An Analytical study has been carried out to develop probable equations to predict the out-of-plane flexural capacity of a TRM-retrofitted URM wall. Different equations are available in the current literature for TRM contribution to the retrofitted URM wall under out-of-plane loading. Therefore, Two equations have been considered in the current study, and the accuracy of these equations has been assessed by comparing equations results with experimental results in the database.

This chapter is different from the other parts of the thesis, where the contribution of insulation layers has been ignored, and only the contribution of TRM has been considered in capacity calculations.

3.1 Formulations to calculate capacity of TRM retrofitted masonry walls

According to the literature review, Two equations have been studied in the current study to calculate the out-of-plane flexural capacity of a TRM-retrofitted URM wall as follows:

Expressions by (D'Antino et al., 2018)

This equation provided accurate prediction as mentioned in the literature review; therefore it has been adopted in the current study for more investigations. In this approach, TRM behaviour derived from TRM characterisation bond tests on a masonry substrate to calculate the greatest flexural strength using enforcing the cross-section rotation equilibrium, considering that plain sections stay plane during loading, which requires a perfect bond at all material interfaces. More details are described by (D'Antino et al., 2018).

$$M_{DA} = f'_m . L_m . k_1 c . \left(\frac{t_m}{2} - k_2 . c\right) + A_f . E_f . \varepsilon_{ffe} . \left(\frac{t_m + t_c}{2}\right) \quad \text{......................... (3.1)}$$

$$k_1 = 1000\varepsilon_m \left(0.5 - \frac{1000}{12}\varepsilon_m\right), if\ \varepsilon_m \leq \varepsilon_{m1} \quad \text{......................... (3.2)}$$

$$k_1 = 1 - \frac{2}{3000\varepsilon_m}, if\ \varepsilon_{m1} \leq \varepsilon_m \leq \varepsilon_{mu} \quad \text{......................... (3.3)}$$

$$k_2 = \frac{8 - 1000\varepsilon_m}{4(6 - 1000\varepsilon_m)}, if\ \varepsilon_m \leq \varepsilon_{m1} \quad \text{......................... (3.4)}$$

$$k_2 = \frac{1000\varepsilon_m (3000\varepsilon_m - 4) + 2}{2000\varepsilon_m (3000\varepsilon_m - 2)}, if\ \varepsilon_{m1} \leq \varepsilon_m \leq \varepsilon_{mu} \quad \text{......................... (3.5)}$$

$$c = \frac{A_f . E_f . \varepsilon_{ffe}}{f'_m . L . k_1} \quad \text{......................... (3.6)}$$

Where ε_m: the masonry strain in the compressed edge equal to 0.0035 for clay masonry and to 0.0025 for concrete masonry, ε_{m1}: the strain associated with the end of the parabolic shape = 0.0020, ε_{mu}: masonry maximum compressive strain =0.0035, c: the neutral axis depth, k_1 and k_2 are the coefficients that define the stress block associated to the parabolic rectangle distribution of the masonry compressive stresses, A_f: cross-sectional area of fibres in the TRM, E_f: tensile modulus of elasticity of TRM, ε_{ffe}: effective tensile strain in TRM, f'_m: compressive strength of masonry, L_m: length of masonry wall, t_m: thickness of masonry wall, t_c: TRM thickness.

Based Equation (3.1), k_1 and k_2 depend on the cross-section strain distribution. k_1 is related to f'_m, so it affects the values of compressive strength of masonry, while k_2 is related to c, so it affects the values the neutral axis depth.

Expressions by (Bajpai and Duthinh., 2013)

A simple equation has been adopted in the current study created by (Bajpai and Duthinh., 2003) for FRP-strengthened structures to calculate the out-of-plane flexural capacity of TRM-retrofitted URM walls. This approach needs equilibrium of forces as in Equation 3.7; thus the ultimate moment can determine by considering reinforcement ruptures before masonry crushes as in Equation 3.8.

$$0.80^2\, f'_m . L_m . z = A_f . E_f . \varepsilon_{ffe} \qquad \text{........................ (3.7)}$$

$$M_{BA} = A_f . E_f . \varepsilon_{ffe} . (t_m - 0.40\, z) \qquad \text{........................ (3.8)}$$

Where z: distance from extreme compression fibre to neutral

3.2 Experimental Database

This part displays the values and distribution of the parameters of masonry walls and TRM systems in the experimental database. The database including 108 URM walls retrofitted using TRM techniques and underwent out-of-plane loading has been collected from the literature. The URM walls exhibited in the database by thirteen studies that investigated various parameters (Bernat-Maso et al., 2014) (Babaeidarabad, 2013) (Valluzzi et al., 2014) (Carozzi et al., 2015) (Bellini et al., 2017) (Bellini et al., 2018) (Gattesco and Boem, 2017) (Padalu et al., 2018) (Shermi and Dubey, 2017) (Dong et al., 2020) (Kariou al., 2018) (Turco et al., 2006) (Harajli et al.,2010). Three walls were enhanced on two sides, and to anchor the

TRM retrofitting, GFRP connectors (anchorages) passed by the walls and were coated using epoxy glue (Gattesco and Boem, 2017).

3.2.1 Parameters of Masonry walls

Table 3.1 shows the parameters of retrofitted URM walls in the database in terms of the dimension of wall $b \times l_m \times t_m$, where l is the distance between supports, the type of wall units (full and hollow clay bricks, concrete masonry units, rubble stone, and cobblestone), and compressive strength of masonry, units and bond mortar.

a) Compressive strength of wall Ingredients:

As in Figure 3.1, the value of compressive strength for masonry f'_m is less than 10 MPa for most of the specimens (71%), while values of compressive strength for masonry units f'_{unit} range from 20 to 30 MPa for more than half of the samples. Bonding mortar for units has a compressive strength f'_{mortar} of less than 10 MPa for 67% of specimens.

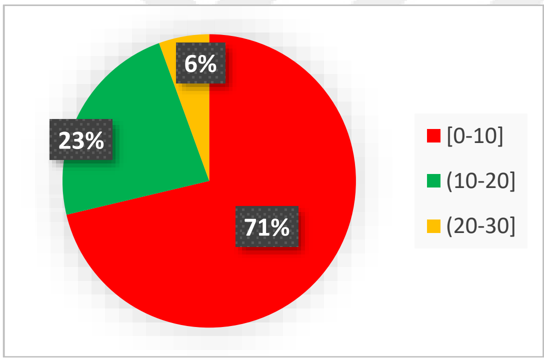

(a)

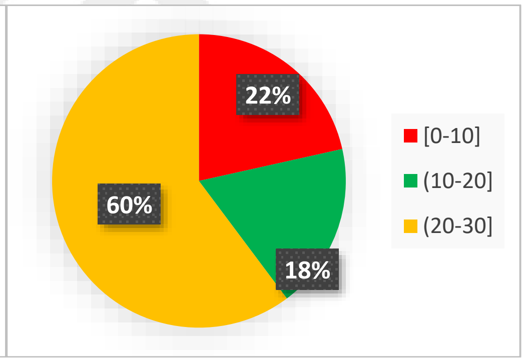

(b)

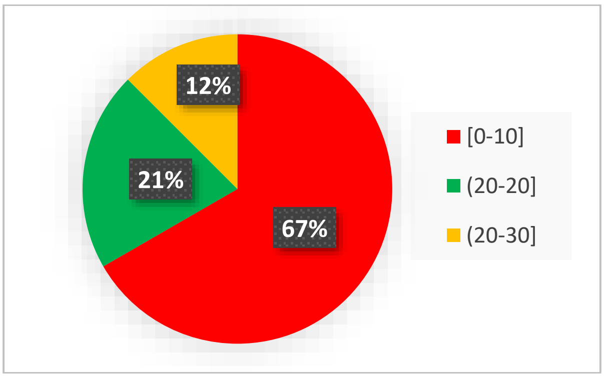

(c)

Figure 3.1 Distribution of compressive strength for wall ingredients, a) masonry wall b) masonry units c) mortar (unites in MPa)

b) Types of walls:

According to Figure 3.2, an overwhelming of the samples (86%) are composed of clay bricks (CB). In contrast, (12%) of specimens are composed of concrete masonry units

(CMU) and are investigated by two study groups. Therefore, TRM systems appear especially suitable for retrofitting heritage masonry structures which are generally composed of full clay bricks or for retrofitting existing infill walls of concrete frame structures, which were generally created of hollow clay bricks (HCB). Because of the difficulty in producing the specimens of TRM-strengthened stone masonry (rubble stone (RS) and cobblestone (CS)), very few samples of stone units are in the database (D'Antino et al., 2018).

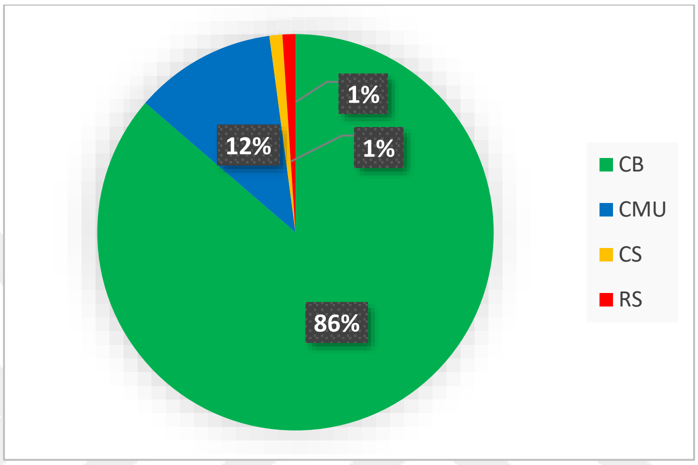

Figure 3.2 Distribution of masonry type

c) Distance between supports l_m: According to Figure 3.3, half of the walls (50%) are small-scale specimens with 1000< l_m ≤2000 mm, and a limited percentage (7%) of specimens have a distance between supports of 2000< l_m ≤3000 mm.

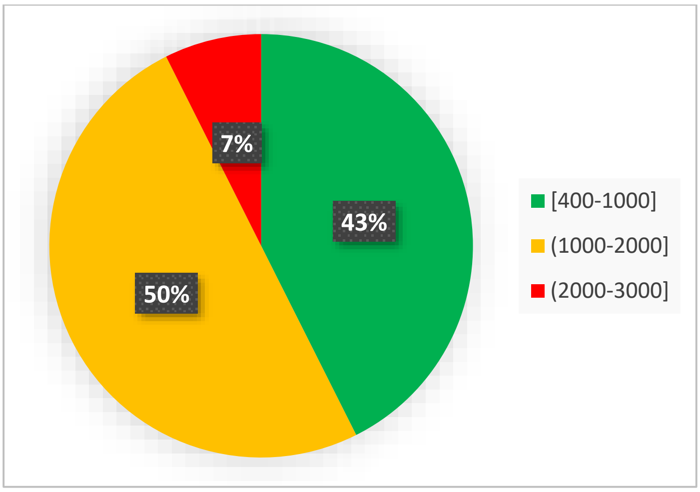

Figure 3.3 Distribution of distance between supports (units in mm)

d) Wall thickness t_m: Most of the thicknesses of specimens (42%) are 100 < t_m ≤ 200 mm. In contrast, a tiny percentage of samples (2%) are t_m >300 mm, as in Figure 3.4.

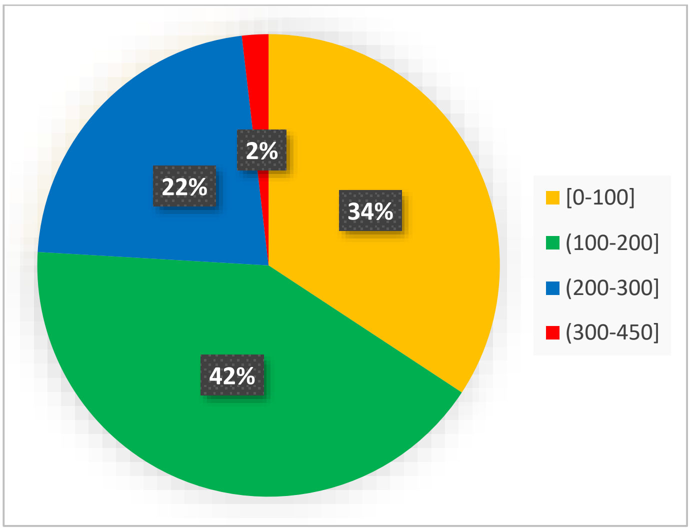

Figure 3.4 Distribution of masonry thickness (units in mm)

Table 3.1 Parameters of masonry wall used in tests

Ref.	Specimen	Masonry type	f'_{unit} MPa	f'_{mortar} MPa	f'_m MPa	b_m mm	l_m mm	t_m mm
Bernat-Maso at., 2014	MGM-11-1	CB	27.9	3.7	10.8	280	560	132
	MGM-11-2	CB	27.9	3.7	10.8	280	560	132
	MGM-11-3	CB	27.9	3.7	10.8	280	560	132
	MGR-11-1	CB	27.9	3.7	10.8	280	450	132
	MGR-11-2	CB	27.9	3.7	10.8	280	560	132
	MGR-11-3	CB	27.9	3.7	10.8	280	560	132
	MCX-11-1	CB	27.9	3.7	10.8	280	560	132
	MCX-11-2	CB	27.9	3.7	10.8	280	560	132
	MCX-11-3	CB	27.9	3.7	10.8	280	560	132
	MGO-11-1	CB	27.9	3.7	10.8	280	450	132
	MCO-11-1	CB	27.9	3.7	10.8	280	450	132
	MSO-11-1	CB	27.9	3.7	10.8	280	450	132
	SGO-11-1	CB	27.9	3.7	10.8	280	450	132
	SCO-11-1	CB	27.9	3.7	10.8	280	450	132
	SSO-11-1	CB	27.9	3.7	10.8	280	450	132
	SBO-11-1	CB	27.9	3.7	10.8	280	450	132
	SBO-12-1	CB	27.9	3.7	10.8	280	450	132
	SGO-12-1	CB	27.9	3.7	10.8	280	450	132
	SGO-21-1	CB	27.9	3.7	10.8	280	450	132
Babaeidarabad et al., 2014	CMU_1_1	CMU	19	22	19.5	1220	1220	92
	CMU_1_2	CMU	19	22	19.5	1220	1220	92
	CMU_1_3	CMU	19	22	19.5	1220	1220	92

	CMU_4_1	CMU	19	22	19.5	1220	1220	92
	CMU_4_2	CMU	19	22	19.5	1220	1220	92
	CMU_4_3	CMU	19	22	19.5	1220	1220	92
	CL_1_1	HCB	24	22	24.5	1220	1220	92
	CL_1_2	HCB	24	22	24.5	1220	1220	92
	CL_1_3	HCB	24	22	24.5	1220	1220	92
	CL_4_1	HCB	24	22	24.5	1220	1220	92
	CL_4_2	HCB	24	22	24.5	1220	1220	92
	CL_4_3	HCB	24	22	24.5	1220	1220	92
Valluzzi et al., 2014	SRGmag	HCB	3.53	4.14	1.8	390	1100	120
	SRGmag	HCB	3.53	4.14	1.8	390	1100	120
	SRGmag	HCB	3.53	4.14	1.8	390	1100	120
	SRGcem	HCB	3.53	4.14	1.8	390	1100	120
	SRGcem	HCB	3.53	4.14	1.8	390	1100	120
	SRGcem	HCB	3.53	4.14	1.8	390	1100	120
	BTRM	HCB	3.53	4.14	1.8	390	1100	120
	BTRM	HCB	3.53	4.14	1.8	390	1100	120
	BTM	HCB	3.53	4.14	1.8	390	1100	120
	Pent	HCB	3.53	4.14	1.8	390	1100	120
	Pent	HCB	3.53	4.14	1.8	390	1100	120
	Pent	HCB	3.53	4.14	1.8	390	1100	120
Carozzi at.,2015	SB_PBO_1	CB	na	na	8.6	315	570	100
	SB_PBO_2	CB	na	na	8.6	315	570	100
	SB_PBO_3	CB	na	na	8.6	315	570	100
	SB-PBO-G-1	CB	na	na	8.6	315	570	100
	SB-PBO-G-2	CB	na	na	8.6	315	570	100
	SB-PBO-G-3	CB	na	na	8.6	315	570	100
	HB_PBO_1	HCB	na	na	4.7	380	570	80
	HB_PBO_2	HCB	na	na	4.7	380	570	80
	HB_PBO_3	HCB	na	na	4.7	380	570	80
	HB-PBO-G-1	HCB	na	na	4.7	380	570	80
	HB-PBO-G-2	HCB	na	na	4.7	380	570	80
	HB-PBO-G-3	HCB	na	na	4.7	380	570	80
(Bellini et al., 2017a)	GFRCM1	CB	18.64	0.99	4.0	1200	2700	250
	GFRCM2	CB	18.64	0.99	4.0	1200	2700	250
	GFRCM3	CB	18.64	0.99	4.0	1200	2700	250
	GFRCM_01	CB	22.07	0.99	4.0	1185	2675	250

(Bellini et al., 2017b)	SRG_01	CB	18.64	0.99	4.0	1185	2675	250
Gattesco and Boem, 2017	BB-1-R	CB	44.0	5.1	7.9	1000	2840	280
	BR-1-R	RS	na	5.1	4.5	1000	2840	435
	BC-0-R	CS	na	3.1	1.0	1000	2840	445
Padaluet al., 2018	SD-25-1	CB	26.16	14.75	7.62	490	1020	250
	SD-25-2	CB	26.16	14.75	7.62	488	1020	252
	SD-25-3	CB	26.16	14.75	7.62	485	1020	250
	SD-25-4	CB	26.16	14.75	7.62	484	1020	252
	SL-25-1	CB	26.16	14.75	7.62	482	1020	255
	SL-25-2	CB	26.16	14.75	7.62	479	1020	252
	SL-25-3	CB	26.16	14.75	7.62	485	1020	250
	SL-25-4	CB	26.16	14.75	7.62	480	1020	250
	SD-50-1	CB	26.16	14.75	7.62	483	1020	250
	SD-50-2	CB	26.16	14.75	7.62	484	1020	250
	SD-50-3	CB	26.16	14.75	7.62	485	1020	252
	SD-50-4	CB	26.16	14.75	7.62	480	1020	248
	SL-50-1	CB	26.16	14.75	7.62	480	1020	250
	SL-50-2	CB	26.16	14.75	7.62	480	1020	247
	SL-50-3	CB	26.16	14.75	7.62	487	1020	246
	SL-50-4	CB	26.16	14.75	7.62	489	1020	250
Shermi and Dubey, 2017	RMFST-12	CB	10	2.5	4.0	500	1000	230
	RMFST-15	CB	10	2.5	4.0	500	1000	230
Dong et al., 2020	WC1-1	CB	25.3	4.98	5.3	235	720	115
	WC1-2	CB	25.3	4.98	5.3	235	720	115
	WC1-3	CB	25.3	4.98	5.3	235	720	115
	WG3-1	CB	25.3	4.98	5.3	235	720	115
	WG3-2	CB	25.3	4.98	5.3	235	720	115
	WG3-3	CB	25.3	4.98	5.3	235	720	115
Kariouet al., 2018	S_C1	CB	21.2	6.54	9.7	440	1125	103
	S_C1_(Co)	CB	21.2	8.86	9.7	440	1125	102.5
	S_G3	CB	21.2	6.54	9.7	440	1125	102.5
	S_G3_(Co)	CB	21.2	8.86	9.7	440	1125	102.5
	S_G7	CB	21.2	7.73	9.7	440	1125	102.5
	S_B3	CB	21.2	7.73	9.7	440	1125	102.5
	D_C1	CB	21.2	6.59	9.7	440	1125	102.5
	D_G3	CB	21.2	6.68	9.7	440	1125	102.5

Turco et al., 2006	CO2-GC26-CB	CB	10.5	7.6	2.7	610	1220	100
	CO2-GC36-CB	CB	10.5	7.6	2.7	610	1220	100
	CO2-GC19-CS	CB	10.5	7.6	2.7	610	1220	100
	CO2-GC29-CS	CB	10.5	7.6	2.7	610	1220	100
	CO2-GC19-CB	CB	10.5	7.6	2.7	610	1220	100
	CO2-GC-29-CB	CB	10.5	7.6	2.7	610	1220	100
Harajli et al.,2010	HB-G-LN	CMU	7	9	2.1	400	1000	100
	HB-G-LH	CMU	7	9	2.1	400	1000	100
	HB-G-TYFO	CMU	7	9	2.1	400	1000	100
	HB-WM1-LH	CMU	7	9	2.1	400	1000	100
	HB-WM1-TYFO	CMU	7	9	2.1	400	1000	100
	Br-G-LH	CB	20	9	4.2	400	1000	100
	Br-G-TYFO	CB	20	9	4.2	400	1000	100

3.2.2 Parameters of TRM composite

The TRM characteristics have been adopted in this study in terms of TRM stress-strain behaviour based on results of bond and tensile tests as in the approach of (D'Antino et al.,2018) where the TRM stress-strain behaviour is assumed composite depending on the outcomes of bond tests (single- or double-lap shear tests, bending tests, or pull-out tests) on TRM strips are used to the particular substrate considered and of tensile testing on the component that debonds (referred to as the debonding component). In particular, the study of (D'Antino et al.,2018) and (D’Antino et al.,2022) have been adopted to obtain the values of elastic modulus of the debonding part E_f, and the effective tensile strain ε_{ffe}.

Table 3.2 presents the TRM parameters in the database in terms of types of fibre, including the open grid textile (carbon, glass, basalt, steel, PBO, mixed PBO, and glass); types of TRM matrix (lime-based, cementitious, pozzolanic, mixed cement, and lime, magnesia); and a number of fibre textile layers n. The distribution of TRM parameters in the database is presented as follows:

a) Types of textile and matrix: Figure 3.5 illustrates that glass (36%), carbon (21%), and basalt (20%) fibres are used most frequently to manufacture textiles, respectively. In contrast, cementitious mortar for specimens (71%) is used most often to manufacture TRM matrix.

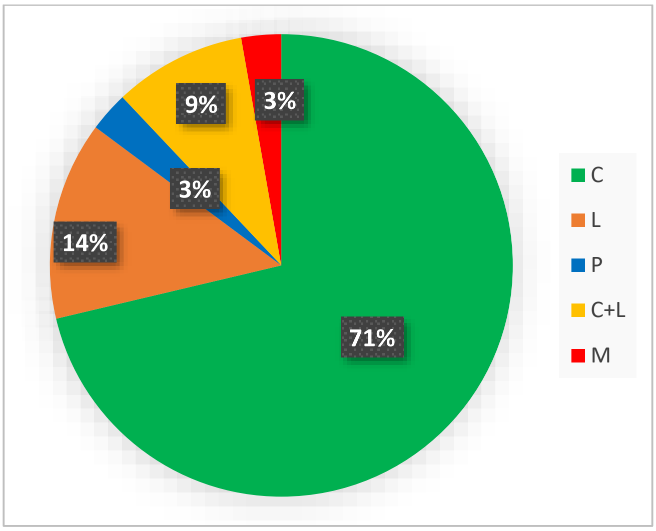

Figure 3.5 Distribution of matrix type

b) Compressive strength of matrix: According to Figure 3.6, most values of compressive strength for the matrix are in the range of 10-20Mpa (35%), 30-40Mpa (21%), and 0–10Mpa (19%), respectively.

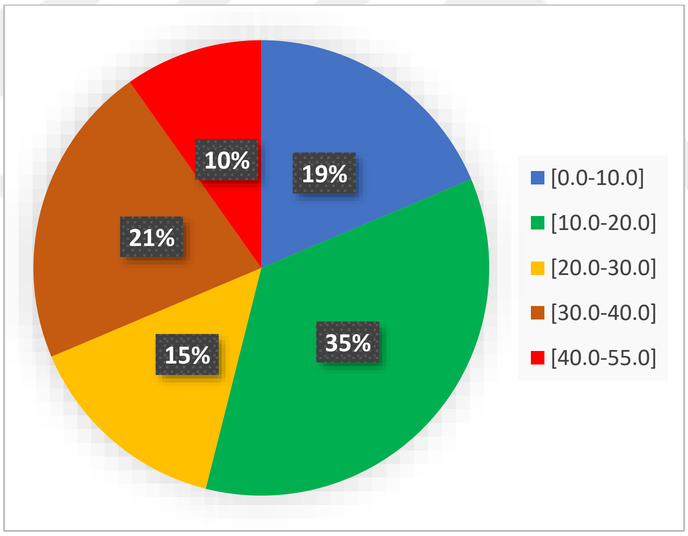

Figure 3.6 Distribution of matrix compressive strength (units in MPa)

c) Number of textile layers n: 81% of the specimens are TRM systems with only one textile layer, and the maximum TRM layers are used with seven textile layers, as in Figure 3.7.

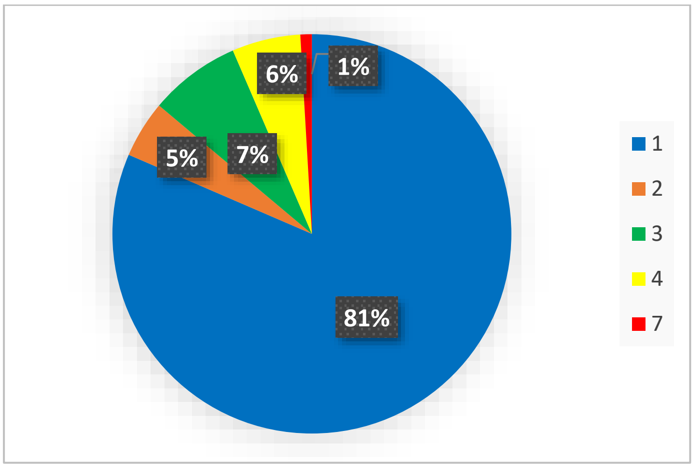

Figure 3.7 Distribution the number of TRM layers

d) Textile equivalent thickness t_f: The thickness of 56% of the specimens ranges from 0.035 to 0.060 mm^2/mm, as in Figure 3.8.

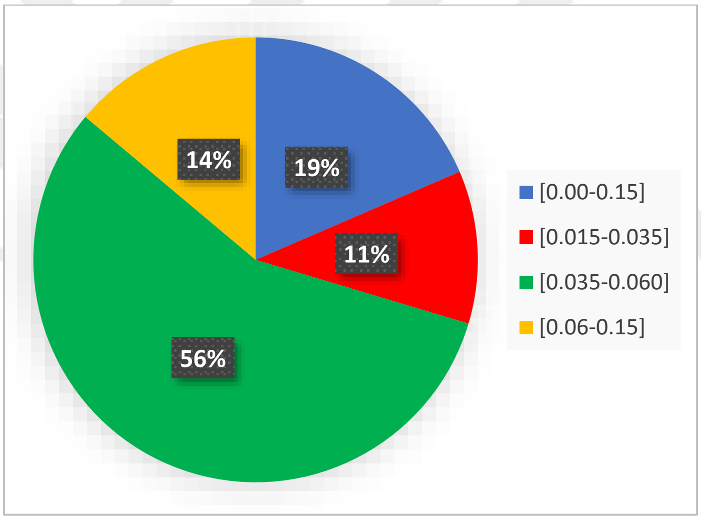

Figure 3.8 Distribution of textile equivalent thickness (units in mm)

Table 3.2 Parameters of TRM composites

Ref.	Specimen	Matrix type	f_{cm}	Textile type	n	t_f mm	A_f mm^2	E_f Gpa	ε_{ffe} %
Bernat-Maso at., 2014	MGM-11-1	C	42.20	G	1	0.04	11.2	90	1.11
	MGM-11-2	C	42.20	G	1	0.04	11.2	90	1.11
	MGM-11-3	C	42.20	G	1	0.044	12.32	90	1.11
	MGR-11-1	L	14.50	G	1	0.04	11.2	90	1.11
	MGR-11-2	L	14.50	G	1	0.04	11.2	90	1.11
	MGR-11-3	L	14.50	G	1	0.044	12.32	90	1.11
	MCX-11-1	P	34.50	C	1	0.049	13.72	240	0.61
	MCX-11-2	P	34.50	C	1	0.049	13.72	240	0.61

	MCX-11-3	P	34.50	C	1	0.05	14.00	240	0.61
	MGO-11-1	C+L	4.60	G	1	0.044	12.32	90	1.11
	MCO-11-1	C+L	4.60	C	1	0.045	12.60	240	0.61
	MSO-11-1	C+L	4.60	S	1	0.057	15.96	190	0.76
	SGO-11-1	C+L	4.60	G	1	0.044	12.32	90	1.11
	SCO-11-1	C+L	4.60	C	1	0.045	12.60	240	0.61
	SSO-11-1	C+L	4.60	S	1	0.057	15.96	190	0.76
	SBO-11-1	C+L	4.60	B	2	0.033	9.24	95	1.05
	SBO-12-1	C+L	4.60	B	2	0.033	18.48	95	1.05
	SGO-12-1	C+L	4.60	G	2	0.044	24.64	90	1.11
	SGO-21-1	C+L	4.60	G	1	0.044	12.32	90	1.11
Babaeidarabad et al., 2014	CMU_1_1	C	20.00	C	1	0.048	58.60	203	0.56
	CMU_1_2	C	20.00	C	1	0.048	58.60	203	0.56
	CMU_1_3	C	20.00	C	1	0.048	58.60	203	0.56
	CMU_4_1	C	20.00	C	4	0.048	234.24	203	0.56
	CMU_4_2	C	20.00	C	4	0.048	234.24	203	0.56
	CMU_4_3	C	20.00	C	4	0.048	234.24	203	0.56
	CL_1_1	C	20.00	C	1	0.048	58.56	203	0.56
	CL_1_2	C	20.00	C	1	0.048	58.56	203	0.56
	CL_1_3	C	20.00	C	1	0.048	58.56	203	0.56
	CL_4_1	C	20.00	C	4	0.048	234.24	203	0.56
	CL_4_2	C	20.00	C	4	0.048	234.24	203	0.56
	CL_4_3	C	20.00	C	4	0.048	234.24	203	0.56
Valluzzi et al., 2014	SRGmag	M	23.86	S	1	0.011	4.29	190	1.16
	SRGmag	M	23.86	S	1	0.011	4.29	190	1.16
	SRGmag	M	23.86	S	1	0.011	4.29	190	1.16
	SRGcem	C	35.16	S	1	0.011	4.29	190	1.26
	SRGcem	C	35.16	S	1	0.011	4.29	190	1.26
	SRGcem	C	35.16	S	1	0.011	4.29	190	1.26
	BTM	C	35.16	B	1	0.05	20.40	90	1.93
	BTM	C	35.16	B	1	0.05	20.40	90	1.93
	BTM	C	35.16	B	1	0.05	20.40	90	1.93
	Pent	C	35.16	G	1	0.122	47.60	13.8	1.67
	Pent	C	35.16	G	1	0.122	47.60	13.8	1.67
	Pent	C	35.16	G	1	0.122	47.60	13.8	1.67
	SB_PBO_1	C	20.00	PBO	1	0.017	5.30	216	0.92
	SB_PBO_2	C	20.00	PBO	1	0.017	5.30	216	0.92

Carozzi at.,2015	SB_PBO_3	C	20.00	PBO	1	0.017	5.30	216	0.92
	SB-PBO-G-1	C	20.00	PBO+G	1	0.014	4.50	40	2.50
	SB-PBO-G-2	C	20.00	PBO+G	1	0.014	4.50	40	2.50
	SB-PBO-G-3	C	20.00	PBO+G	1	0.014	4.50	40	2.50
	HB_PBO_1	C	20.00	PBO	1	0.014	5.30	216	0.92
	HB_PBO_2	C	20.00	PBO	1	0.014	5.30	216	0.92
	HB_PBO_3	C	20.00	PBO	1	0.014	5.30	216	0.92
	HB-PBO-G-1	C	20.00	PBO+G	1	0.014	5.40	40	2.50
	HB-PBO-G-2	C	20.00	PBO+G	1	0.014	5.40	40	2.50
	HB-PBO-G-3	C	20.00	PBO+G	1	0.014	5.40	40	2.50
(Bellini et al., 2017)	GFRCM1	L	13.09	G	1	0.055	66.00	70	1.51
	GFRCM2	L	12.06	G	1	0.038	45.60	70	1.69
	GFRCM3	L	14.74	G	1	0.035	42.00	72	1.78
(Bellini et al., 2018)	GFRCM_01	L	10.57	G	1	0.051	60.44	65	1.54
	SRG_01	L	15.25	G	1	0.021	24.89	156	1.62
Gattesco and Boem, 2017	BB-1-R	L	6.29	G	1	0.11	110.00	30.04	1.93
	BR-1-R	L	6.29	G	1	0.11	110.00	30.04	1.93
	BC-0-R	L	6.29	G	1	0.11	110.00	30.04	1.93
Padaluet al., 2018	SD-25-1	C	14.75	B	1	0.038	18.62	95	0.9
	SD-25-2	C	14.75	B	1	0.038	18.54	95	0.9
	SD-25-3	C	14.75	B	1	0.038	18.43	95	0.9
	SD-25-4	C	14.75	B	1	0.038	18.39	95	0.9
	SL-25-1	C	14.75	B	1	0.038	18.32	95	1.2
	SL-25-2	C	14.75	B	1	0.039	18.68	95	1.2
	SL-25-3	C	14.75	B	1	0.038	18.43	95	1.2
	SL-25-4	C	14.75	B	1	0.039	18.72	95	0.9
	SD-50-1	C	14.75	B	1	0.042	20.29	95	1.2
	SD-50-2	C	14.75	B	1	0.042	20.3	95	1.2
	SD-50-3	C	14.75	B	1	0.042	20.37	95	1.2
	SD-50-4	C	14.75	B	1	0.043	20.64	95	1.2
	SL-50-1	C	14.75	B	1	0.043	20.64	95	1.2
	SL-50-2	C	14.75	B	1	0.043	20.64	95	1.2
	SL-50-3	C	14.75	B	1	0.042	20.45	95	1.2
	SL-50-4	C	14.75	B	1	0.042	20.54	95	1.2
Shermi and Dubey, 2017	RMFST-12	C	2.50	S	1	0.126	63.00	149	0.5
	RMFST-15	C	2.50	S	1	0.129	64.50	149	0.5
	WC1-1	C	51.94	C	1	0.056	13.16	239	0.7

Dong et al., 2020	WC1-2	C	51.94	C	1	0.056	13.16	239	0.7
	WC1-3	C	51.94	C	1	0.056	13.16	239	0.7
	WG3-1	C	51.94	G	3	0.011	7.76	71	3.5
	WG3-2	C	51.94	G	3	0.011	7.76	71	3.5
	WG3-3	C	51.94	G	3	0.011	7.76	71	3.5
Kariouet al., 2018	S_C1	C	38.36	C	1	0.097	42.68	225	0.7
	S_C1_(Co)	C	37.30	C	1	0.097	42.68	225	0.7
	S_G3	C	38.36	G	3	0.044	58.08	74	1.9
	S_G3_(Co)	C	37.25	G	3	0.044	58.08	74	1.9
	S_G7	C	37.39	G	7	0.044	135.52	74	1.9
	S_B3	C	37.39	B	3	0.037	48.84	89	1.5
	D_C1	C	41.49	C	1	0.097	42.68	225	0.7
	D_G3	C	46.58	G	3	0.044	58.08	74	1.9
Turco et al., 2006	CO2-GC26-CB	C	na	G	2	0.054	65.88	50.163	1.6
	CO2-GC36-CB	C	na	G	3	0.054	98.82	50.163	1.4
	CO2-GC19-CS	C	na	G	1	0.136	82.96	40.8	1.6
	CO2-GC29-CS	C	na	G	2	0.136	165.92	40.8	1.6
	CO2-GC19-CB	C	na	G	1	0.136	82.96	40.8	1.6
	CO2-GC-29-CB	C	na	G	2	0.136	165.92	40.8	1.6
Harajli et al.,2010	HB-G-LN	Lim	5.50	G	1	0.031	12.4	70	1.4
	HB-G-LH	lime	9.00	G	1	0.031	12.4	70	1.4
	HB-G-TYFO	cement	36.00	G	1	0.031	12.4	70	1.4
	HB-WM1-LH	lime	9.00	S	1	0.015	6	190	1.3
	HB-WM1-TYFO	cement	36.00	S	1	0.015	6	190	1.3
	Br-G-LH	lime	9.00	G	1	0.031	12.4	70	1.4
	Br-G-TYFO	cement	36.00	G	1	0.031	12.4	70	1.4

Note: G: glass, C: carbon, PBO: polyparapheny benzopesoxazole, B: Basalt, MT: matrix type, C: cementitious, L: lime-based, M1: high-ductility hydraulic mortar and P: pozzolanic, na: not available.

3.3 Results of equations predictions

An analytical moment capacity has been predicted using equations studied in the current study for 64 TRM-retrofitted URM walls exposed to out-of-plane load. To assess the equations accuracy, the equations results have been compared with the experimental results of the flexural capacity of TRM-strengthened masonry walls by statistical analysis. Table 3.3 displays the experimental and analytical moment capacities.

Although the database in the current study contains 108 specimens, the analytical moment capacity has been predicted for 64 specimens because some specimens were subjected to shear failure or failure was not attained and because of the absence of some parameters to calculate the specimens' moment capacity.

Table 3.3 Comparision of experimental and analytical moment capacities

Reference	Specimen	M_{ex} (kN·m)	M_{DA} (kN·m)	M_{BA} (kN·m)
Bernat-Maso at.,2014	MGM-11-1	1.46	1.52	1.46
	MGM-11-2	1.58	1.51	1.46
	MGM-11-3	1.84	1.68	1.61
	MGR-11-1	1.48	1.52	1.46
	MGR-11-2	1.34	1.54	1.46
	MGR-11-3	1.56	1.67	1.61
	MCX-11-2	1.01	2.64	2.61
	MCX-11-3	1.02	2.69	2.66
	MCO-11-1	0.73	2.38	2.39
	MSO-11-1	3.02	3.01	2.97
	SCO-11-1	0.79	2.39	2.39
	SSO-11-1	2.07	2.97	2.97
	SBO-11-1	0.54	1.18	1.21
	SBO-12-1	1.71	2.38	2.39
	SGO-12-1	1.71	3.20	3.17
	SGO-21-1	1.15	1.63	1.61
Babaeidarabad et al., 2014	CMU_1_1	6.09	6.24	6.01
	CMU_1_2	6.35	6.24	6.01
	CMU_1_3	6.99	6.24	6.01
	CL_1_1	6.57	6.26	6.03
	CL_1_2	6.2	6.26	6.03
	CL_1_3	6.4	6.26	6.03
Valluzzi ad et al., 2014	SRGmag	1.24	1.12	1.11
	SRGmag	1.24	1.12	1.11
	SRGmag	1.24	1.12	1.11
	SRGcem	0.71	1.22	1.20
	SRGcem	0.71	1.22	1.20
	SRGcem	0.71	1.22	1.20
	SB_PBO_1	1.64	1.08	1.05

Carozzi at.,2015	SB_PBO_2	1.44	1.08	1.05
	SB_PBO_3	1.47	1.08	1.05
	HB_PBO_1	1.03	0.86	0.82
	HB_PBO_2	1.18	0.86	0.82
	HB_PBO_3	1.17	0.86	0.82
Gattesco and Boem, 2017	BB-1-R	19.69	19.39	17.74
	BR-1-R	37.49	31.04	27.54
	BC-0-R	44.38	31.53	27.52
Padaluet al., 2018	SD-25-1	6.66	4.12	3.96
	SD-25-2	4.94	4.12	3.98
	SD-25-3	5.36	4.05	3.92
	SD-25-4	4.59	4.08	3.94
	SL-25-1	5.9	5.52	5.29
	SL-25-2	5.63	5.53	5.33
	SL-25-3	5.39	5.39	5.22
	SL-25-4	5.08	4.11	3.98
	SD-50-1	6.3	5.93	5.74
	SD-50-2	5.48	5.94	5.75
	SD-50-3	4.56	6.03	5.81
	SD-50-4	6.16	5.96	5.79
	SL-50-1	4.84	6.03	5.84
	SL-50-2	5.44	5.93	5.77
	SL-50-3	4.67	5.84	5.69
	SL-50-4	6.33	6.00	5.81
Shermi and Dubey, 2017	RMFST-12	13.38	10.72	10.45
	RMFST-15	11.4	10.97	10.69
Dong et al., 2020	WC1-1	3.11	2.64	2.45
	WC1-2	2.96	2.64	2.45
	WC1-3	2.29	2.64	2.45
	WG3-1	3.8	2.10	2.16
	WG3-2	4.75	2.10	2.16
	WG3-3	4.22	2.10	2.16
Kariouet al., 2018	S_C1	6.58	6.70	6.66
	S_G3_(Co)	7.26	6.86	7.99
	S_B3	6.53	4.39	6.44

Statistical analysis has been carried out to evaluate the analytical procedures' accuracy by calculating the ratio between the experimental and theoretical ultimate moment for all specimens and each procedure, as in Equation 3.11. The average of ratios values by Equation 3.12, the associated coefficient of variation by Equation 3.13, and the reference coefficient of variation by Equation 3.14 (D'Antino and Triantafillou, 2016) (D'Antino and Pisani, 2017), which gives a measurement of the dispersion of the ratios concerning the perfect match value $R = 1$ (D'Antino et al., 2018), are assessed. Table 3.4 displays the results of the statistical analysis.

$$R_i = \frac{M_{exp,i}}{M^{ii}_i} \qquad \text{……………………} (3.11)$$

$$\bar{R} = \frac{\sum_i^N R_i}{N} \qquad \text{……………………} (3.12)$$

$$\text{CoV} = \sqrt{\frac{\sum_i^N (R_i - \bar{R})^2}{\bar{R}^2 . N}} \qquad \text{……………………} (3.13)$$

$$\text{CoV}_{ref} = \sqrt{\frac{\sum_i^N (R_i - 1)^2}{N}} \qquad \text{……………………} (3.14)$$

R_i: ratio for each specimen, $\bar{R}$: the average of ratios values, $M_{exp,i}$ and M^{ii}_i: experimental and analytical moment respectively, CoV: the associated coefficient of variation, CoV_{ref}: the references coefficient of variation, i: number of specimens, ii: DA, and BA, and N: the number of considered specimens.

Table 3.4 Results of the statistical analysis.

Theoretical formula	$\bar{R}$	CoV(%)	CoV_{ref}(%)
DA	1.04	34.85	36.68
BA	1.08	39.20	42.90

When $\bar{R}$ amounts are higher than 1.0, the proposition produces conservative assessments by generally underestimating the ultimate moment capacity. CoV represents the proposition dispersion of the outcomes, while CoV_{ref} reference the accuracy of the proposition. The results appear that the average ratio values $\bar{R} = 1.04$ and 1.08 for M_{DA} and M_{BA}, respectively; thus, the maximum resisting bending moment is somewhat overstated by both formulations. The results have been obtained using the DA equation, M_{DA} are more overestimated because of a relatively low dispersion concerning the average R (CoV = 34.85%) and the perfect match $R = 1$ ($\text{CoV}_{ref} = 36.68\%$), indicating the more accurate results of the theoretical predictions using this formula.

In this study, the distribution of the ratios and the corresponding normal distribution function have also been extracted using the best fit of the driven outcomes for each expression, as in Figures 3.9 and 3.10. The higher amount of outcomes close to the perfect match line represents the better performance of the model in prediction.

The DA equation and BA equation predict the flexural capacity of upgraded walls with reasonable accuracy where their most values come close to the perfect match line based on Figure 3.9 and 3.10. Therefore, the BA equation could be used to predict flexural strength and it should be noted that the BA equation is very simple compared to the DA equation which requires more parameters.

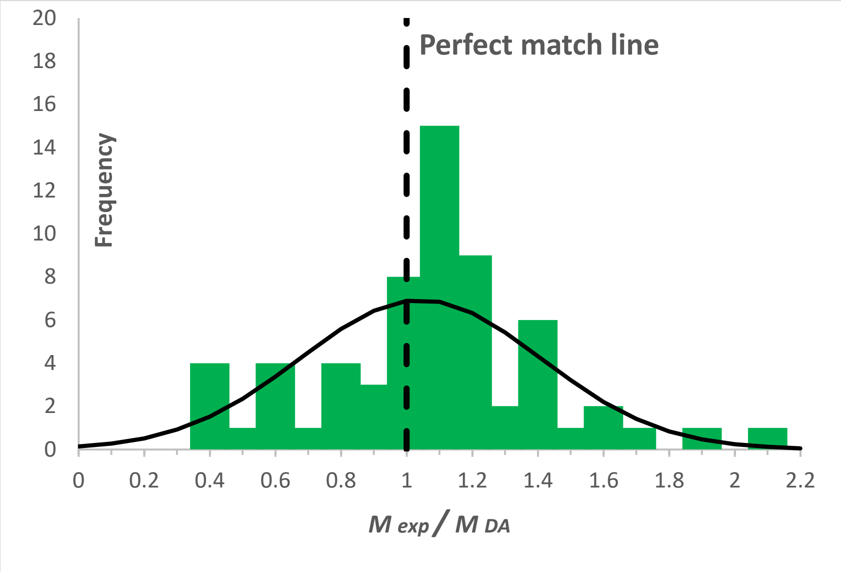

Figure 3.9 Distribution of ratios $R_i = M_{exp,i}/M^{ii}{}_i$ for DA equation

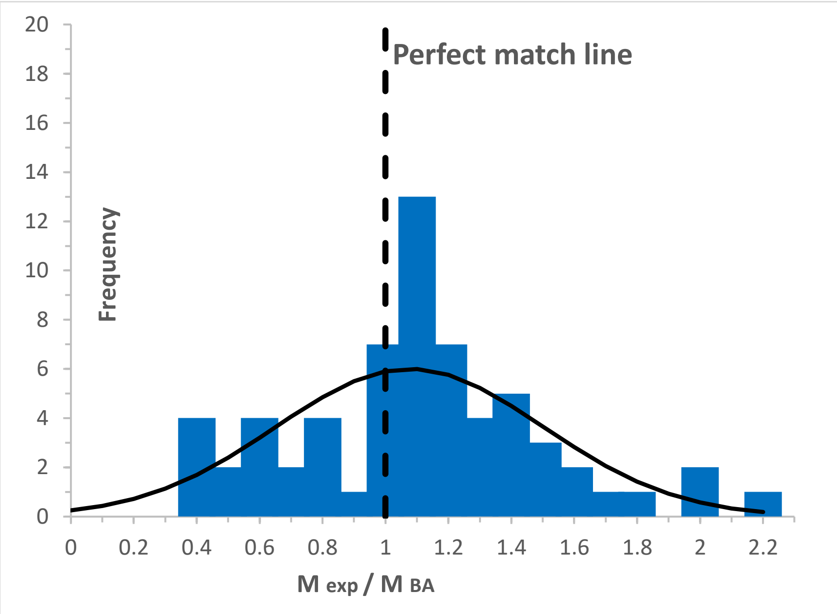

Figure 3.10 Distribution of ratios $R_i = M_{exp,i}/M^{ii}{}_i$ for BA equation

The Calibration of accuracy for formulations results by experimental results versus theoretical results for all formulations as in Figure 3.11. Both formulas reasonably predict the flexural capacity of the retrofitted walls, where most values are close to experimental values.

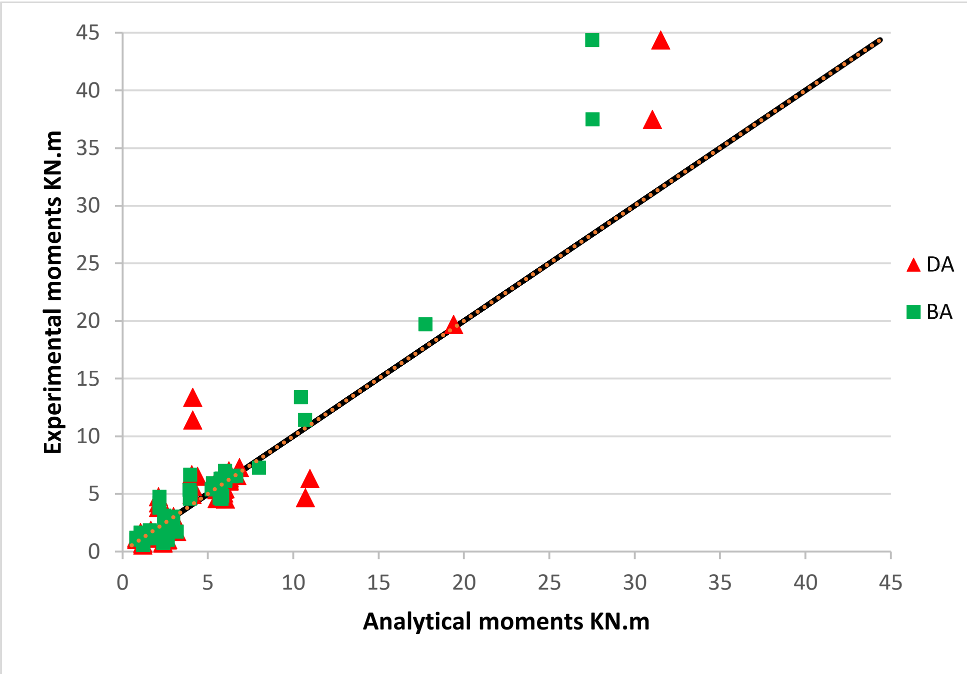

Figure 3.11 Calibration of the accuracy of formulations results

4. FINITE ELEMENT ANALYSIS OF THE RETROFITTED MASONRY WALL

The subject of the current chapter is an investigation of the effectiveness of the finite element (FE) method in predicting the strength and deformation capacity of the retrofitted URM walls in terms of seismic and energy retrofitting. The masonry wall has been retrofitted with TRM material and a thermal insulation panel (TIP). For finite element analysis, Abaqus/CAE 2020 software has been implemented. Concrete damage plasticity (CDP) has been implemented to define the masonry wall and TIP system. The ABAQUS results have been calibrated with the experimental and numerical study results from the literature.

4.1 Introduction

FE techniques are becoming a suitable substitute for experimental tests, so the FE method has become critical. Micro-modelling, simplified micro-modelling and macro-modelling are the methods used in FEM for masonry, where the method is used according to the level of required accuracy and necessary detail (Abdulla et al ., 2017). Figure 4.1 displays micro and simplified micro methods, while Figure 4.2 displays the macro method.

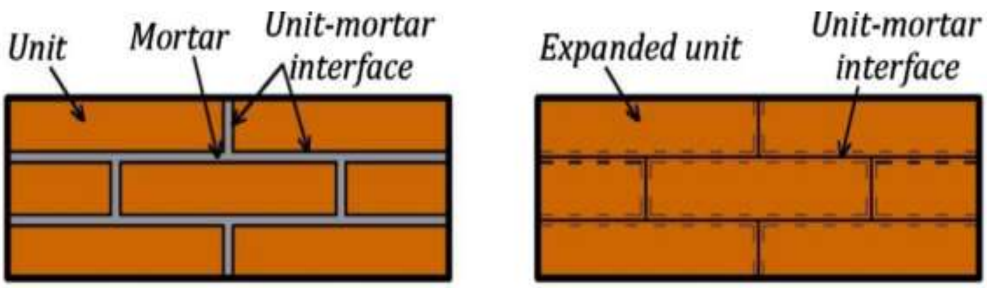

(a) (b)

Figure 4.1 FE techniques: (a) micro technique; (b) simplified micro technique (Lourenço, 1996)

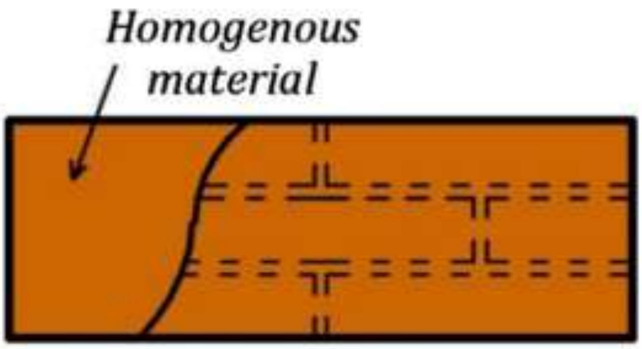

Figure 4.2 Macro-model (Lourenço, 1996)

4.2 Reference Study

The experimental and numerical study carried out by (Karlos et al., 2021) has been adopted to calibrate the results of the FE analysis developed in the current study. Experimental investigations were conducted to retrofit the masonry walls exposed to out-of-plane cyclic loading by implementing TRM material with thermal panels for seismic and thermal retrofitting. The investigations involved a total of 12 wall samples measuring a total of 150 cm in length, 40 cm in width, and 8.5 cm in thickness. The walls were built employing ridge-faced, 12-hole, horizontally perforated clay bricks and masonry mortar for a general purpose. The balanced textile with polymer-coated glass fibre rovings in two perpendicular directions was used, and a cementitious mortar for TRM material. The thermal panels were produced of expanded polystyrene (EPS) panels at a thickness of 2.0 cm. A rigid steel frame was used to apply cyclic out-of-plane loading to all specimens. The brick masonry walls were placed horizontally and then loaded in three-point bending at a span of 130 cm, as in Figure 4.3. Two pairs of steel hinges were positioned at each support along the width of the specimen, at the top and bottom, and a third pair was positioned at mid-span, along the load application line.

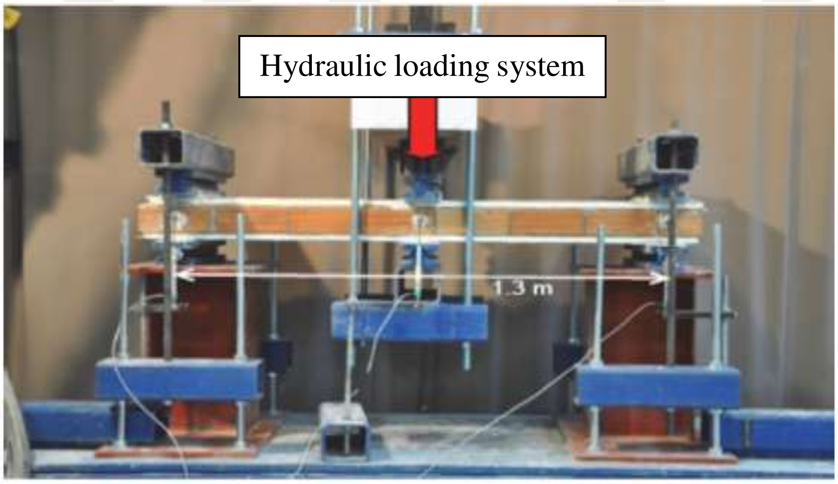

Figure 4.3 The setup of out-of-plane testing in the experiment (Karlos et al., 2021).

The numerical study simulated the experimental tests for brick masonry walls using FE in the ANSYS program. The simulation was monotonic, so load-displacement results numerically produced were compared to envelop curves experimentally produced. The brick wall and the thermal panels were simulated, assuming isotropic homogenous behaviour. In contrast, the TRM was modelled assuming orthotropic membrane behaviour only in the tension state (Karlos et al., 2021).

4.3 Parameters and Geometry

In the FE analysis, five parameters have been considered in the current study: unreinforced masonry wall as control specimen (W), only TRM has been applied to both sides of the wall without TIP (2W2), combining of TRM and TIP to both sides of the wall (1P1W1P1), only TIP has been applied to both sides of the wall without TRM (PWP), and combining of the TRM and TIP to one side of the wall (1P1W). The TIP contribution without the TRM system (PWP specimen) and the contribution of TRM with TIP to one side of the wall (1P1W specimen) have not been investigated in the reference study, so these two parameters have been investigated in the current study. The numbers 1 and 2 indicate the number of layers in the TRM, while the letter P indicates the TIP system. Figure 4.4 presents the cross-section of the five specimens. Figure 4.5 shows masonry wall dimensions, while Figure 4.6 shows the setup for FE analysis and the distance between supports for the control specimen under three-point bending.

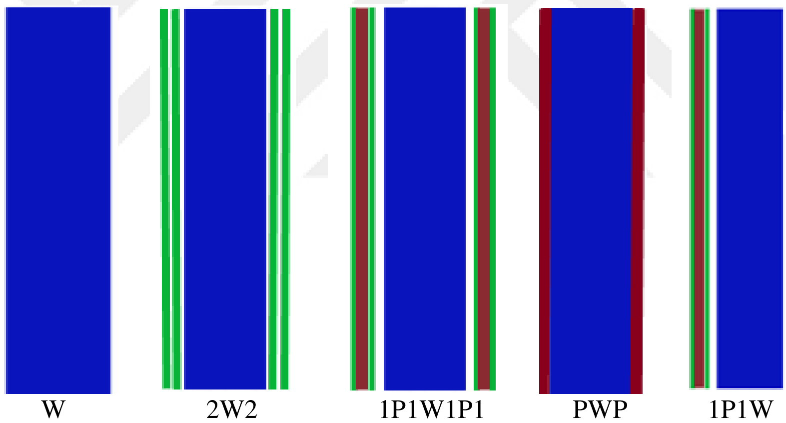

Figure 4.4 Cross-section of original and retrofitted wall specimens

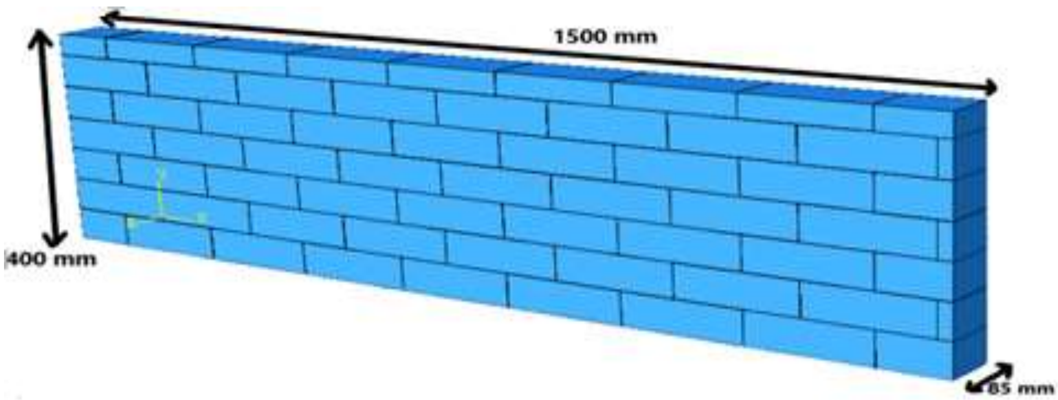

Figure 4.5 3D geometry of masonry wall

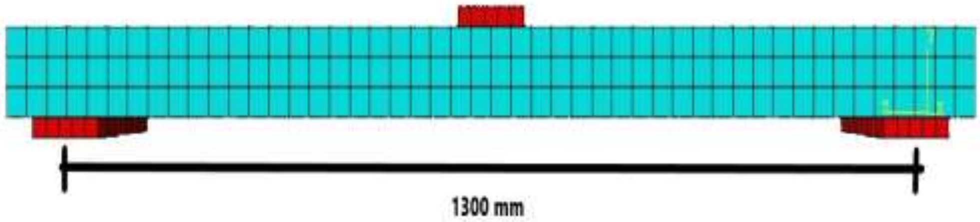

Figure 4.6 Setup for out-of-plane modelling

4.4 Simulations

In this section, simulation procedures have been presented. According to the reference study, the values of damage criteria have not been defined, and all simulations have been stopped after reaching the predetermined displacement levels.

4.4.1 Mechanical Parameters:

Material properties are defined using the many functions in Abaqus. All material properties have been adopted based on reference study. Four materials have been defined in the current study by ABAQUS software as follows:

4.4.1.1 Definition of unreinforced masonry wall

Macro modelling has been adopted to define masonry wall in the ABAQUS program. It has been defined as a homogenised material using concrete-damaged plasticity (CDP) for non-linear behaviour. The stress-strain curve in Figure 4.7 has been adopted for compressive and tension behaviour. The results of experimental investigations on masonry prisms loaded in compression have been adopted for the critical behaviour characteristics. In the case of tension, a fraction of 10% of the compression strength has been suggested based on the reference study (Karlos et al., 2021). Table 4.1 displays the input characteristics of masonry. While Tables 4.2 and 4.3 present the values of non-linear behaviour for masonry in the CDP model based on the reference study.

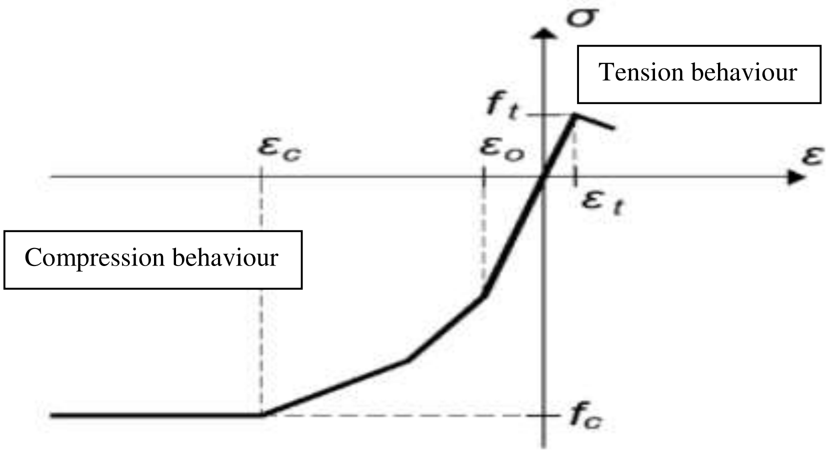

Figure 4.7 Stress-strain curve of masonry in tension and compression (Karlos et al., 2021)

$$E = 1000\sqrt{f'c} \qquad \text{……………………(4.1)}$$

Table 4.1 Input material properties of masonry wall (Karlos et al., 2021)

Mass density tonne/mm^3	2E-09
Young's modulus MPa	11580
Poisson's ratio	0.2
Tensile strength MPa	1.158
Compressive strength MPa	11.58

Table 4.2 Compressive values for masonry in the CDP model

Yield stress (MPa)	Inelastic strain
6.63	0
7.36	0.000473203
7.90	0.000693881
8.35	0.000851508
8.93	0.001072186
9.27	0.001376932
9.56	0.001608119
9.98	0.001965407
10.45	0.002364729
11.03	0.002848119
11.56	0.003299983
11.58	0.003321
11.58	0.005370153
11.58	0.006484051

Table 4.3 Tensile values for masonry in the CDP model

Yield stress (MPa)	Cracking strain
0.3	0

Figure 4.8 presents the definition of the masonry wall in ABAQUS software in terms of density, elastic behaviour and plasticity behaviour by the CDP.

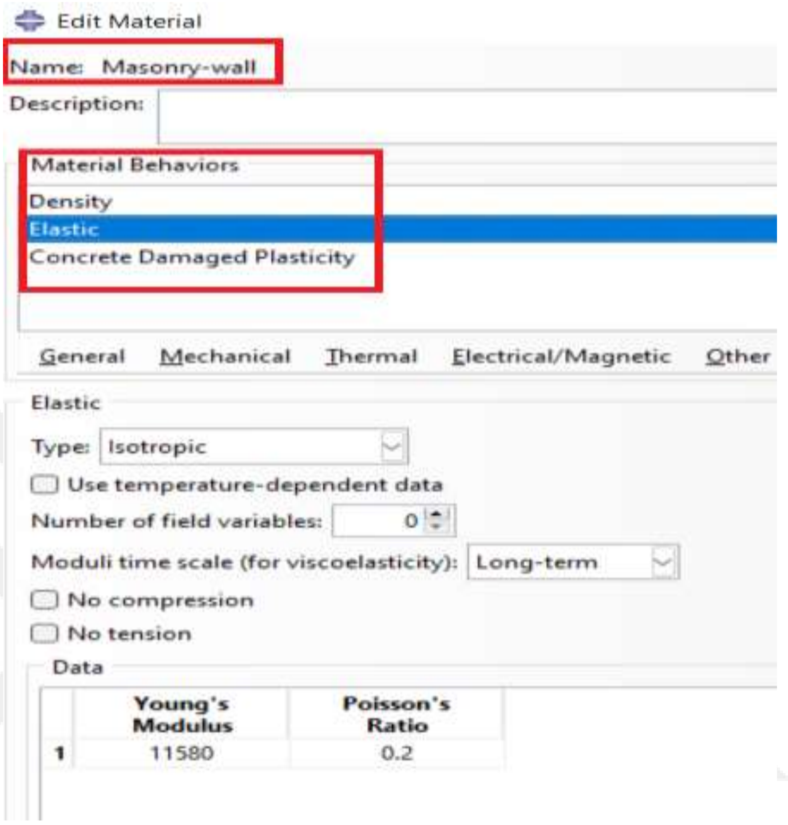

Figure 4.8 Defining masonry in Abaqus

4.4.1.2 Definition of TIP system

TIP has also been defined by employing the concrete damage plasticity (CDP) law. According to the reference study, the stress-strain curve has been adopted for compressive and tension behaviour in Figure 4.9. Table 4.4 shows the input parameters of the TIP. Tables 4.5 and 4.6 present the values of non-linear behaviour for the TIP in the CDP model, based reference study.

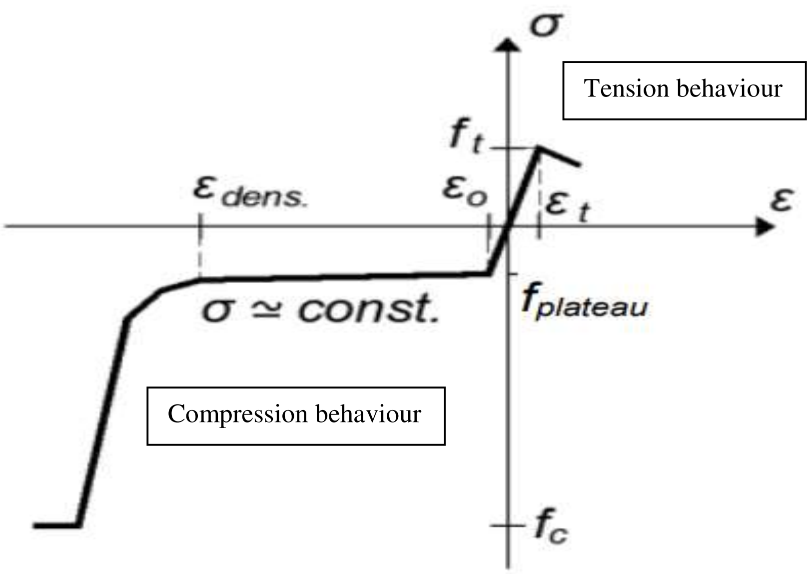

Figure 4.9 Stress-strain curve of the TIP in tension and compression (Karlos et al., 2021)

Table 4.4 Input Parameters of the TIP (Karlos et al., 2021)

Thickness mm	20
Mass density tonne/mm^3	2.9E-10
Young's modulus MPa	20
Poisson's ratio	0.2
Tensile strength MPa	0.3
Compressive strength MPa	1.12
Shear strength MPa	0.125

Table 4.5 Compressive values for the TIP in the CDP model

Yield stress (MPa)	Inelastic strain
0.18	0
0.18	0.000207919
0.18	0.000586174
0.18	0.001645139
0.18	0.002496184
0.18	0.003498486
0.18	0.004008975
0.18	0.004198102
0.18	0.004368669
0.2	0.00452027
0.23	0.004709744
0.24	0.004823532
0.26	0.004937838
0.29	0.005099528
0.33	0.005251879

0.37	0.00530981
0.42	0.005368376
0.52	0.00545657
0.64	0.005573701
0.82	0.005749629
1.06	0.00595553
1.12	0.006023838
1.12	0.006383186
1.12	0.006647884

Table 4.6 Tensile values for the TIP in the CDP model

Yield stress (MPa)	Cracking strain
0.3	0

Figure 4.10 presents the definition of TIP in ABAQUS software in terms of density, elastic behaviour and plasticity behaviour by the CDP.

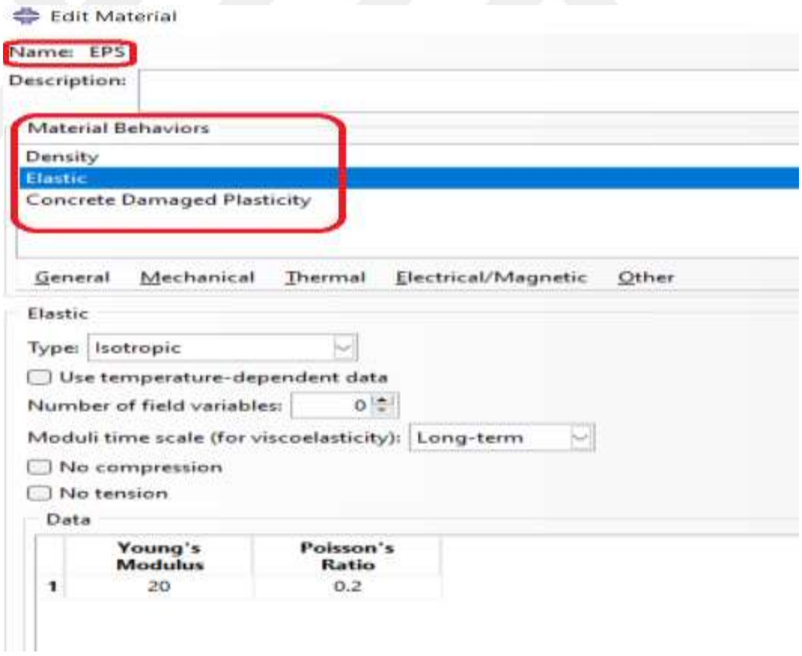

Figure 4.10 Defining the TIP in Abaqus

4.4.1.3 Definition of textile reinforced mortar (TRM)

Plastic material has been used by ABAQUS software to define the non-linear behaviour of the TRM system. Based on the reference study by (Karlos et al., 2021). Figure 4.11 shows the stress-strain curve of the TRM system in tension, while Table 4.7 shows the input parameters of the TRM system. Table 4.8 and Table 4.9 display the values of the plastic case for the TRM system.

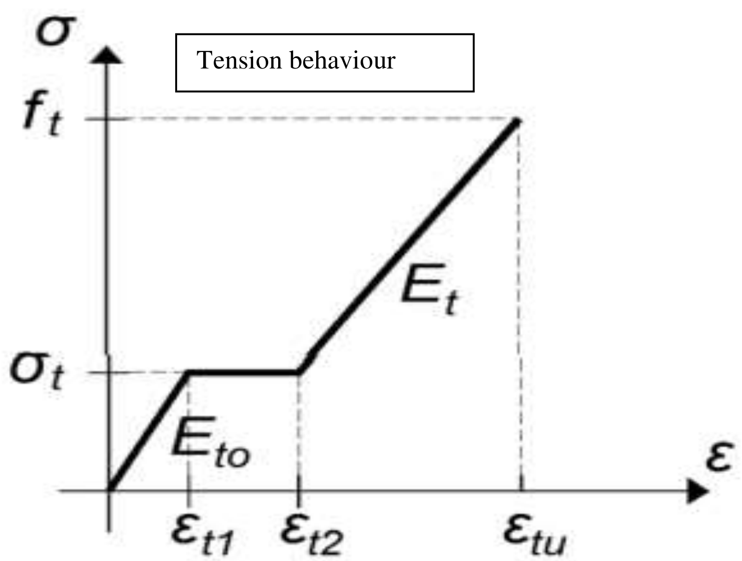

Figure 4.11 Stress-strain curve of TRM composite in tension (Karlos et al., 2021)

Table 4.7 Input parameters of TRM composite (Karlos et al., 2021)

Thickness	1 layer = 5 mm	2 layers = 8 mm
Mass density (tonne/mm^3)	8.7E-10	8.7E-10
Initial stiffness E_{t0} (MPa)	7897	6353
Stress of yielding σ_t (MPa)	3.38	3.85
Strain of yielding ε_{t1}	0.000428	0.000606
Intermediate strain ε_{t2}	0.0075	0.0118
Failure strain ε_u	0.03	0.03
Failure stress f_t (MPa)	9.0	9.0

Table 4.8 Plastic values of TRM-one layers

Yield stress (MPa)	Plastic strain
3.38	0
3.38	0.007072
3.41	0.007172
3.91	0.009172
4.40	0.011172
4.90	0.013172
5.40	0.015172
5.90	0.017172
6.40	0.019172
6.90	0.021172
7.40	0.023172
7.90	0.025172

8.40	0.027172
8.90	0.029172
9	0.029572

Table 4.9 Plastic values of TRM-two layers

Yield stress (MPa)	Plastic strain
3.85	0
3.85	0.011194
3.878296703	0.011294
4.444230769	0.013294
5.010164835	0.015294
5.576098901	0.017294
6.142032967	0.019294
6.707967033	0.021294
7.839835165	0.025294
8.405769231	0.027294
8.971703297	0.029294
9	0.029394

Figures 4.12 and 4.13 present the definition of TRM in ABAQUS software in terms of density, elastic behaviour and plastic behaviour.

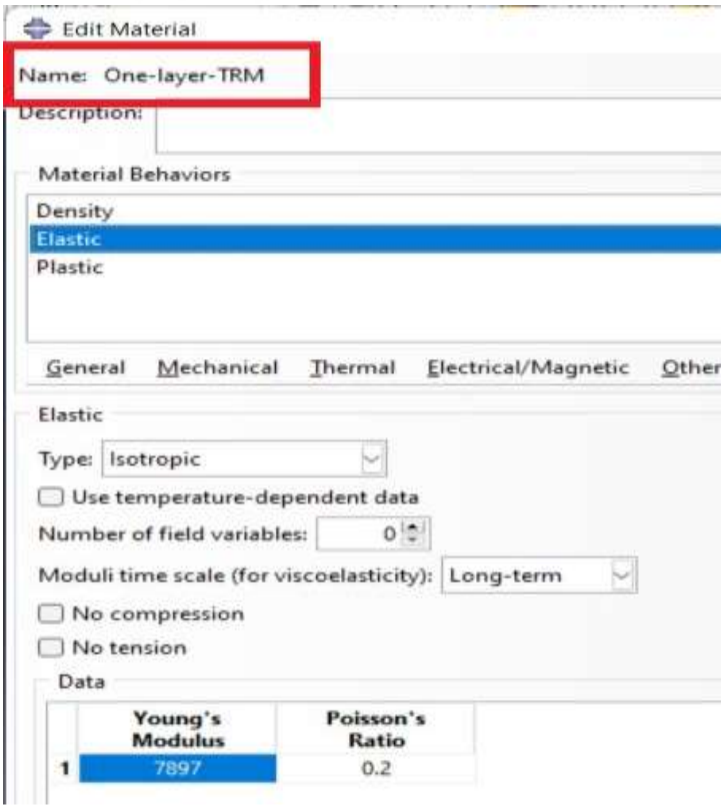

Figure 4.12 Defining one-layer of TRM in Abaqus

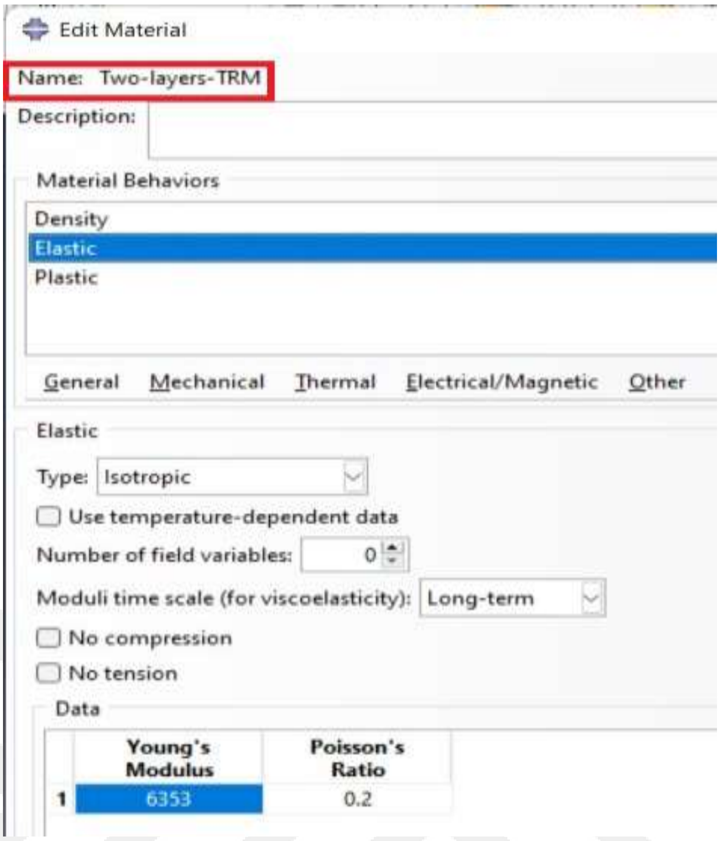

Figure 4.13 Defining two-layers TRM in Abaqus

4.4.2 Models of materials and specimens

A four-part series have been created in the ABAQUS software to simulate the specimens. C3D8R element has been used for walls, steel plates, and TIP. The type of element S4R has been adopted for the TRM composite, as in Figures 4.14, 4.15, 4.16, and 4.17.

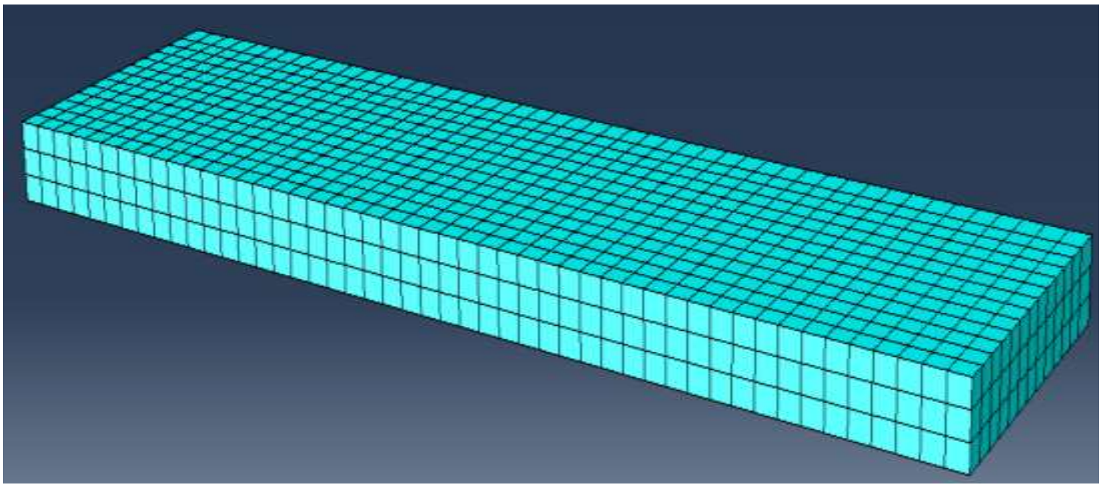
Figure 4.14 Masonry wall part

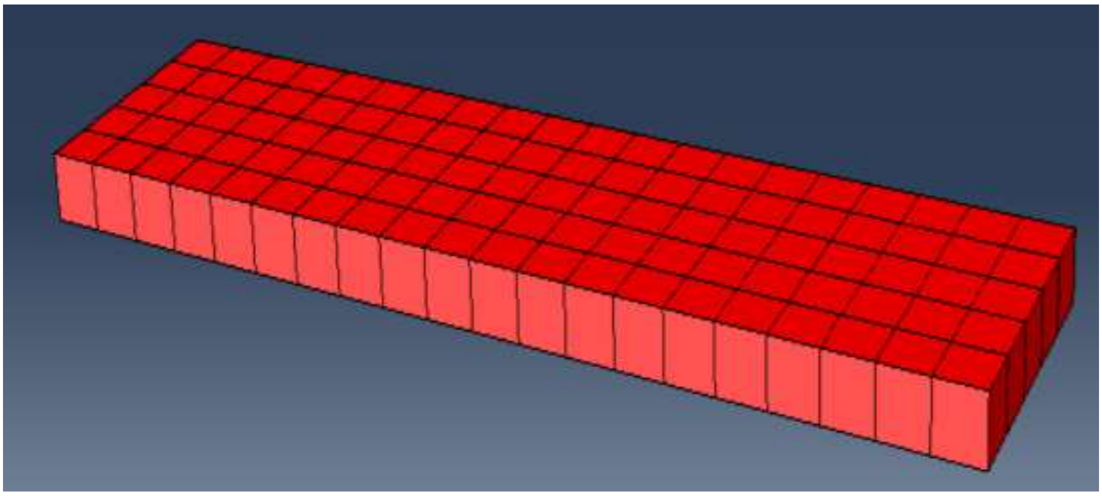
Figure 4.15 Steel part

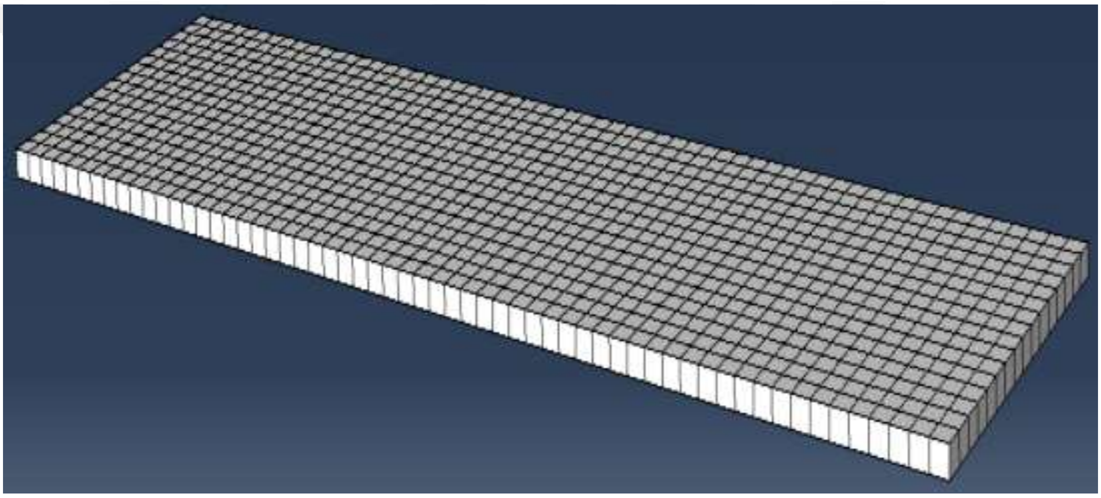
Figure 4.16 TIP part

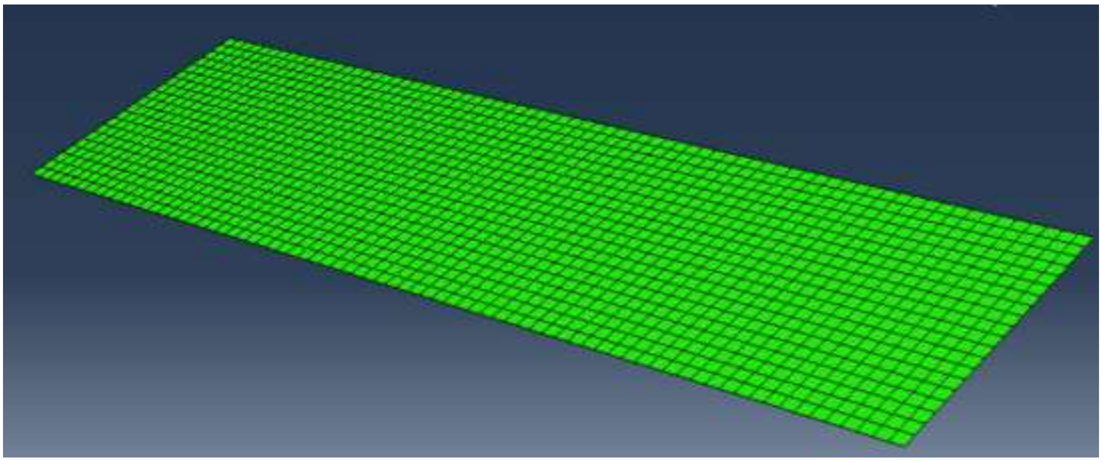
Figure 4.17 TRM part

The finite element model has been implemented for all specimens using the assembly and mesh module of material models, as shown in below Figures.

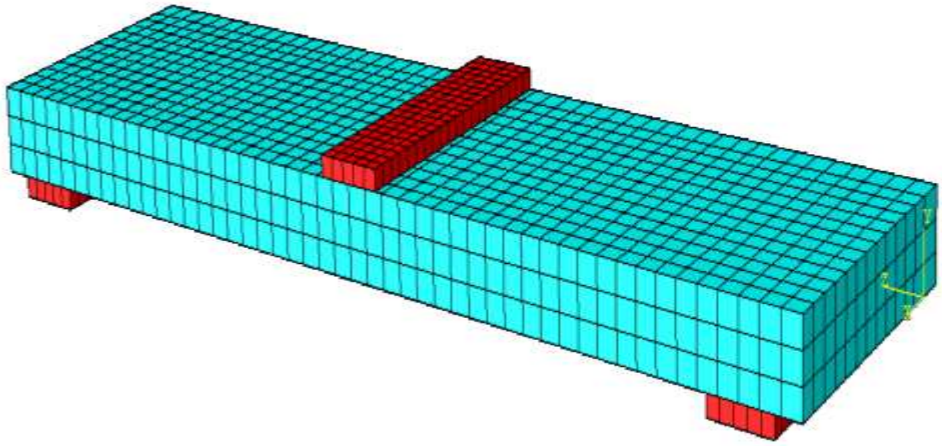

Figure 4.18 Assembly and mesh for W specimen by ABAQUS

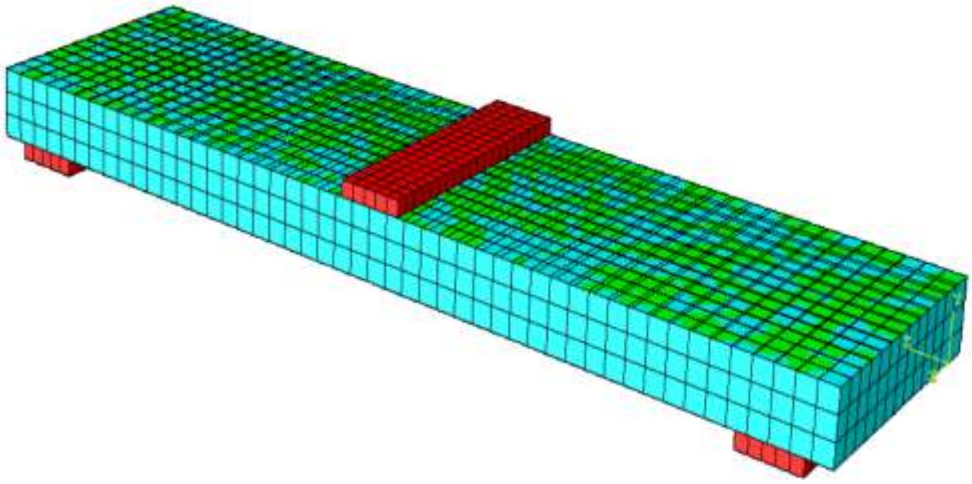

Figure 4.19 Assembly and mesh for 2W2 specimen by ABAQUS

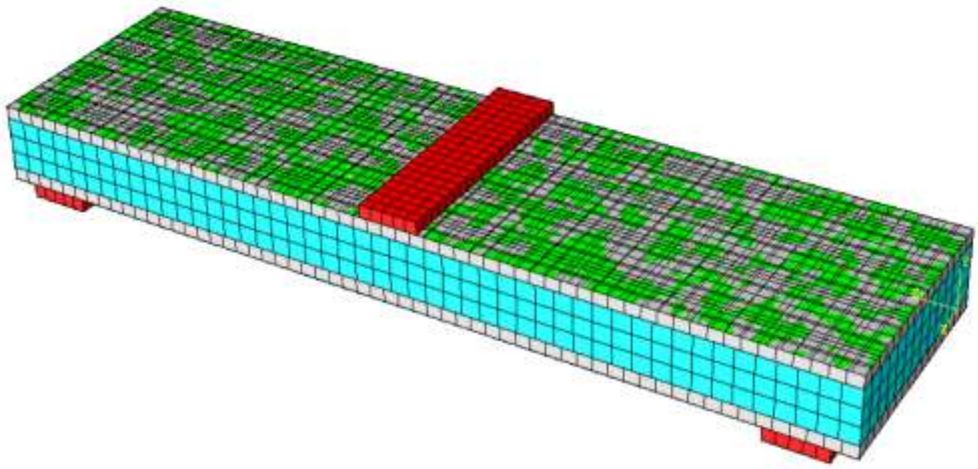

Figure 4.20 Assembly and mesh for 1P1W1P1 specimen by ABAQUS

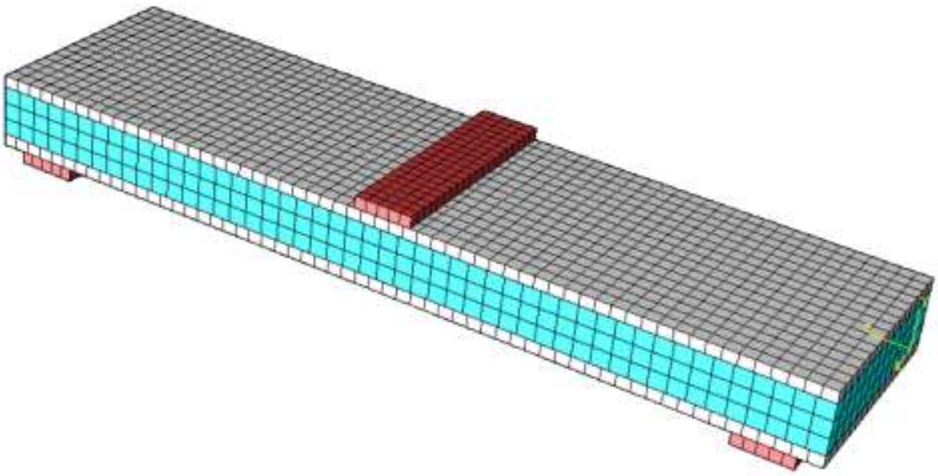

Figure 4.21 Assembly and mesh for PWP specimen by ABAQUS

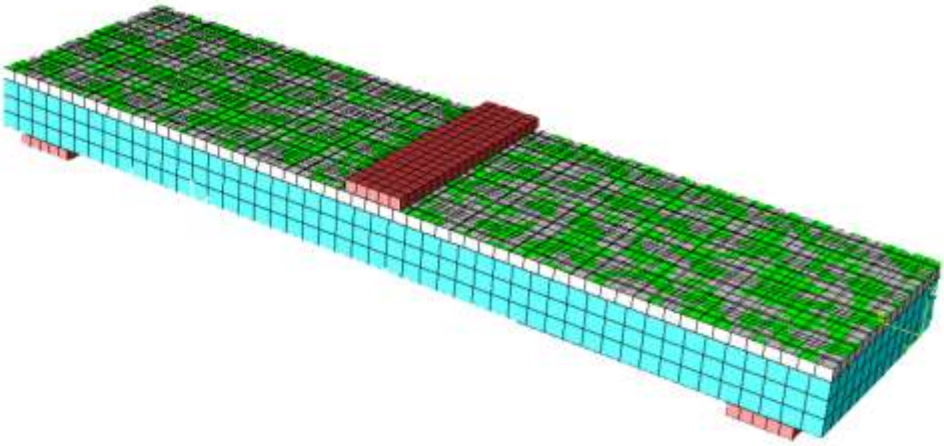

Figure 4.22 Assembly and mesh for 1P1W specimen by ABAQUS

4.4.3 Boundary conditions

The type of boundary conditions has been selected as displacement-rotation for specimens and applied in the right and left plates as in Figures 4.23 and 4.24. In contrast, the type of load has been defined as a displacement for specimens and applied on the top plate according to the reference study as in Figure 4.25.

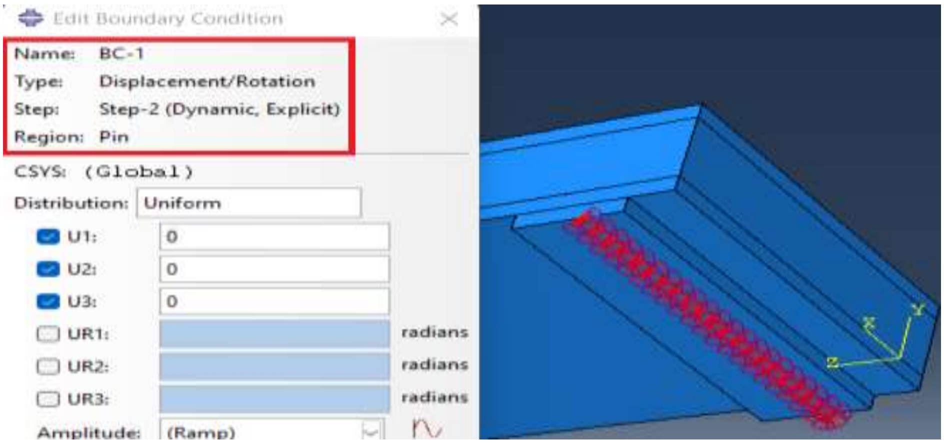

Figure 4.23 Boundary condition of the right steel plate

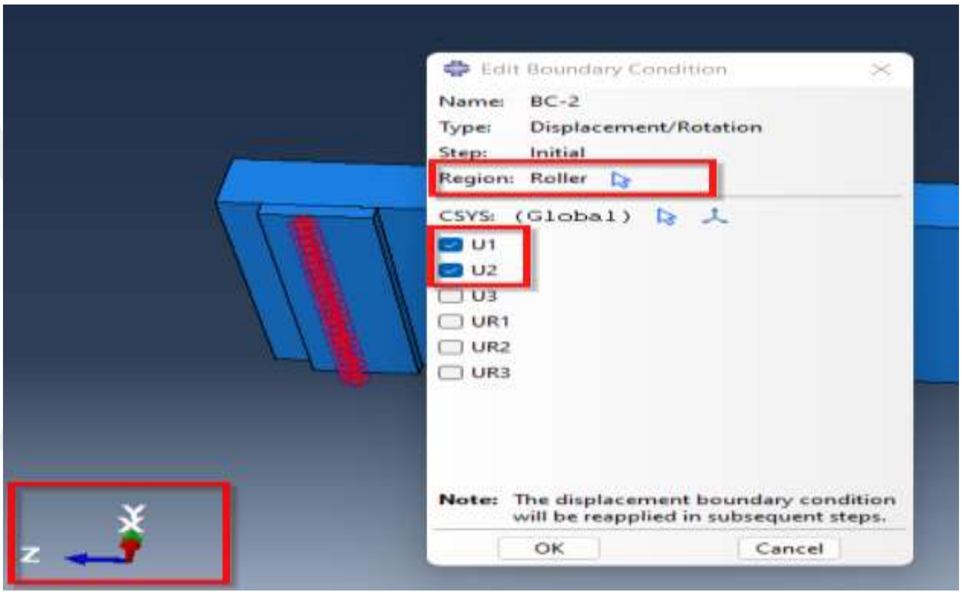

Figure 4.24 Boundary condition of the left steel plate

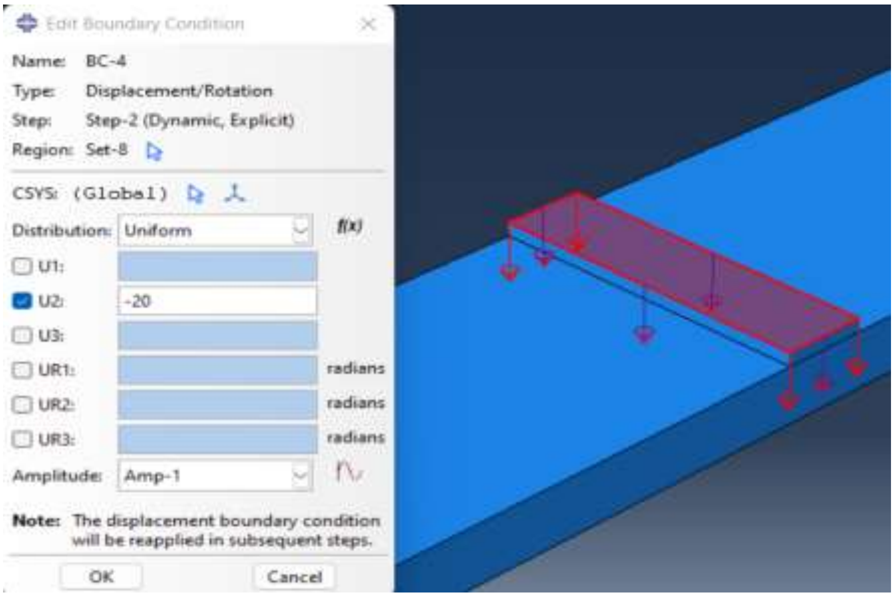

Figure 4.25 Boundary condition of the top steel plate for 2W2 specimen

4.4.4 Interaction

The contact between parts of a model has been implemented for each specimen on both sides. The below Figures present the constraints of parts for the 1P1M1P1 specimen on the load side.

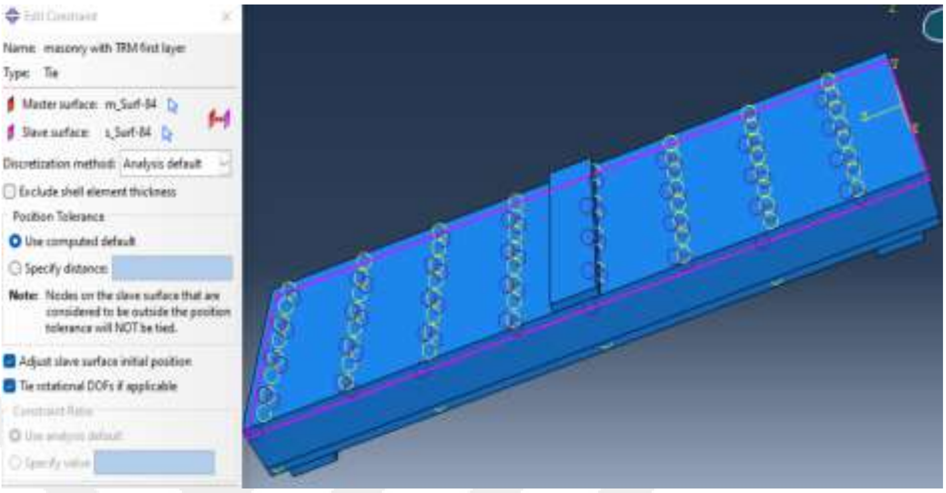

Figure 4.26 Constraint of masonry with TRM first layer

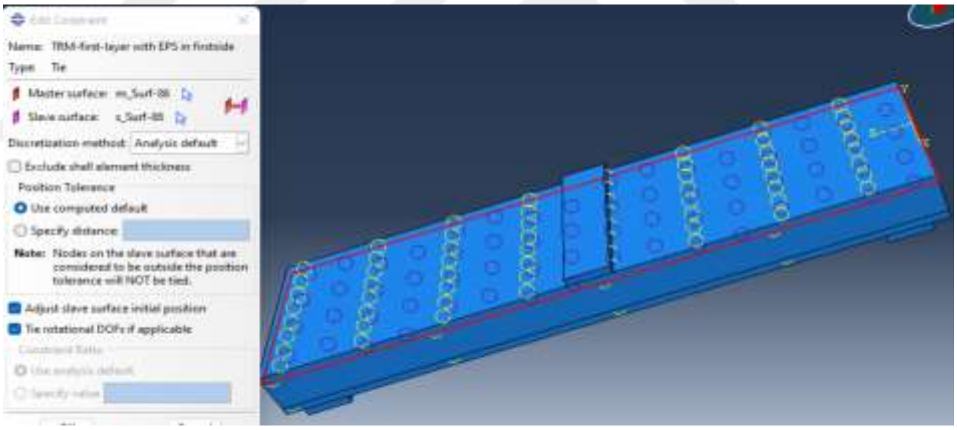

Figure 4.27 Constraint of TRM first layer with TIP

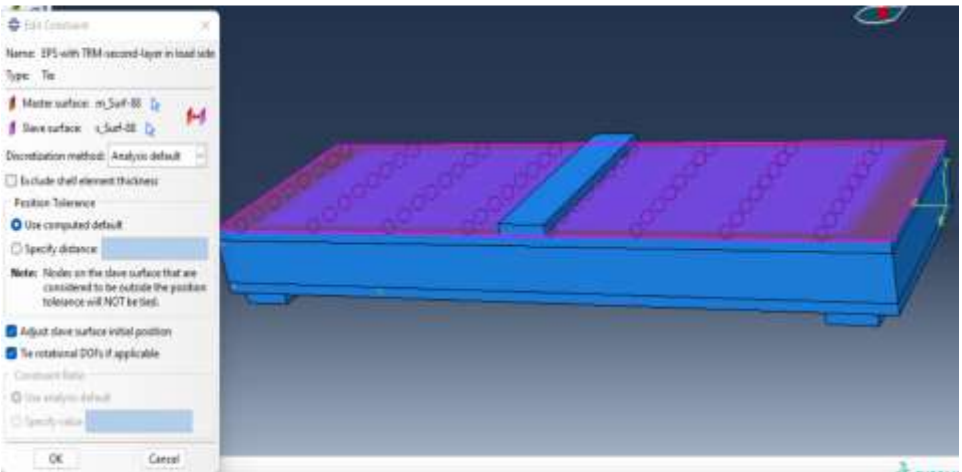

Figure 4.28 Constraint of TIP with TRM second layer

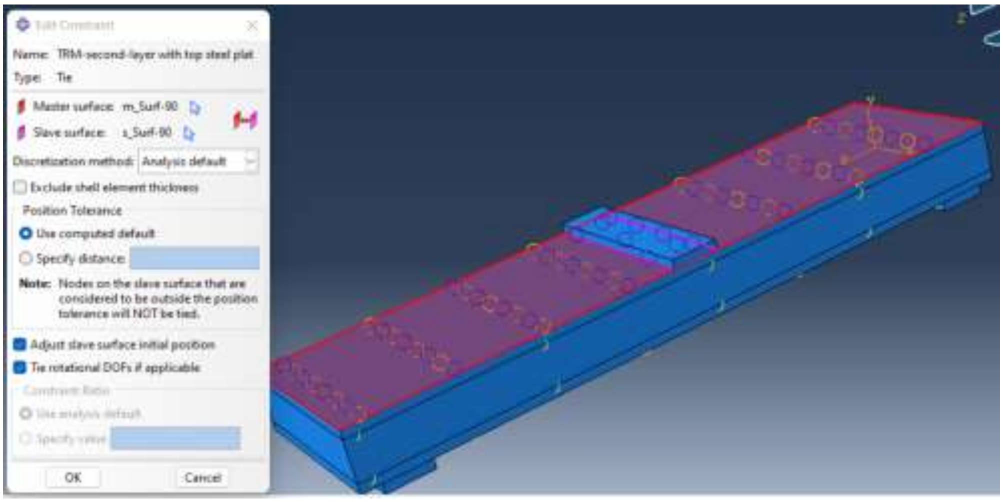

Figure 4.29 Constraint of TRM second layer with top of steel plate

4.4.5 Step

By step module, the results have been outputted by ABAQUS software in the current work as in below Figures.

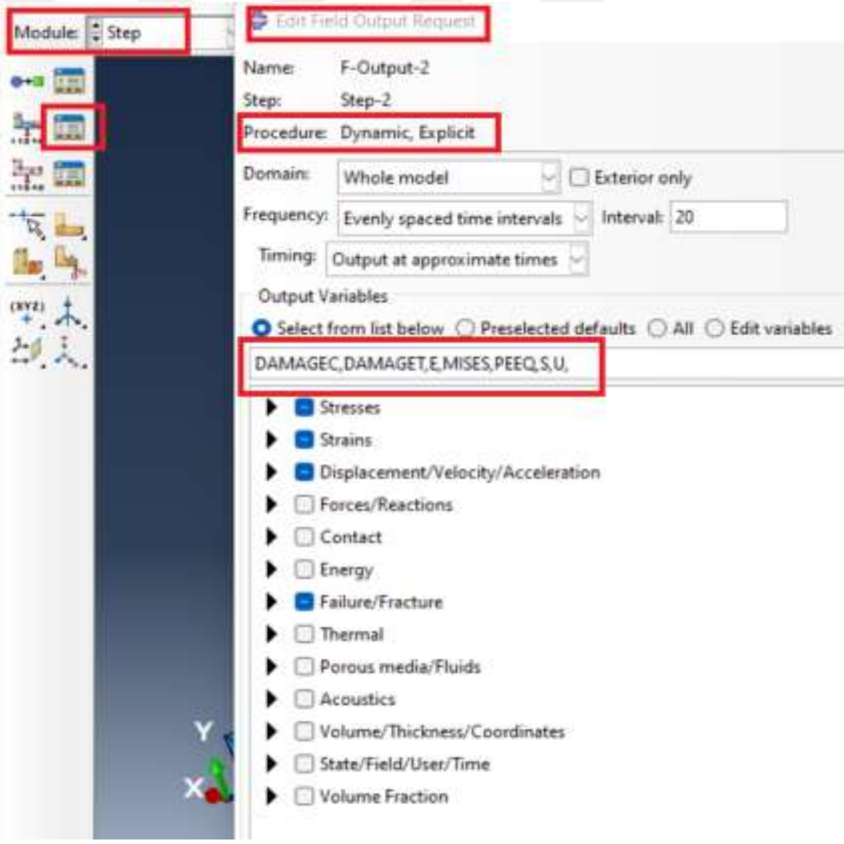

Figure 4.30 Outputted results for all specimens

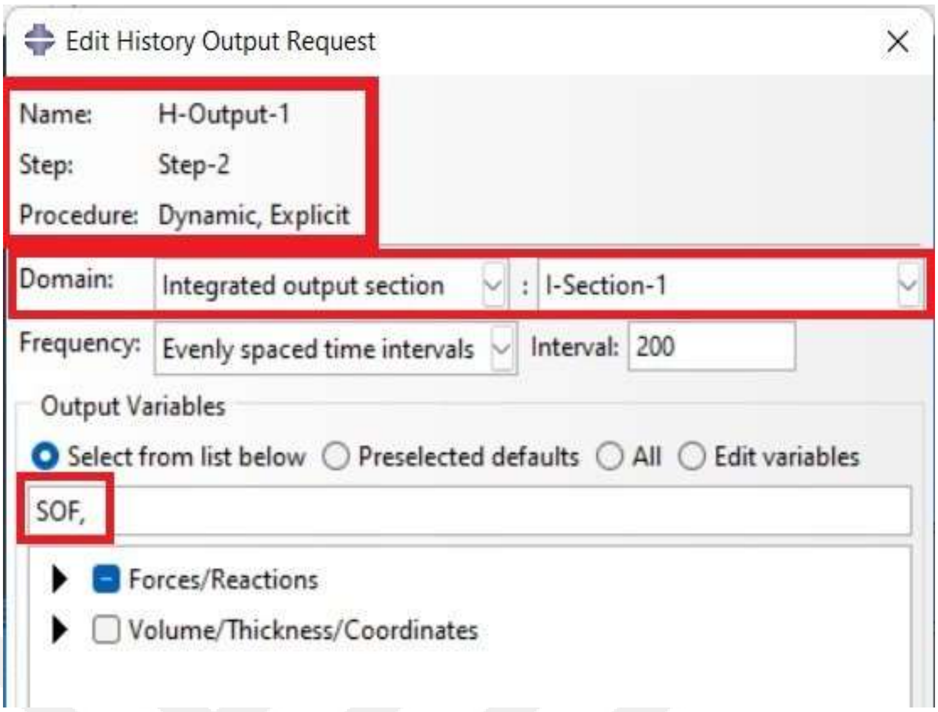

Figure 4.31 The outputting of forces values for fir integrated output section

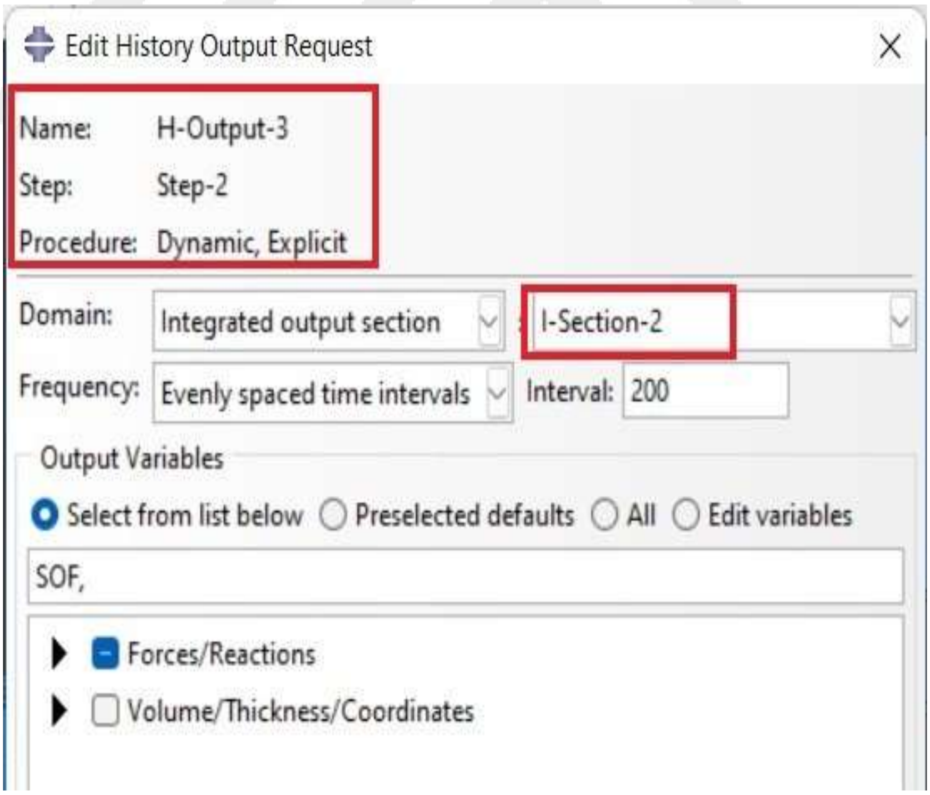

Figure 4.32 The outputting of forces values for second integrated output section

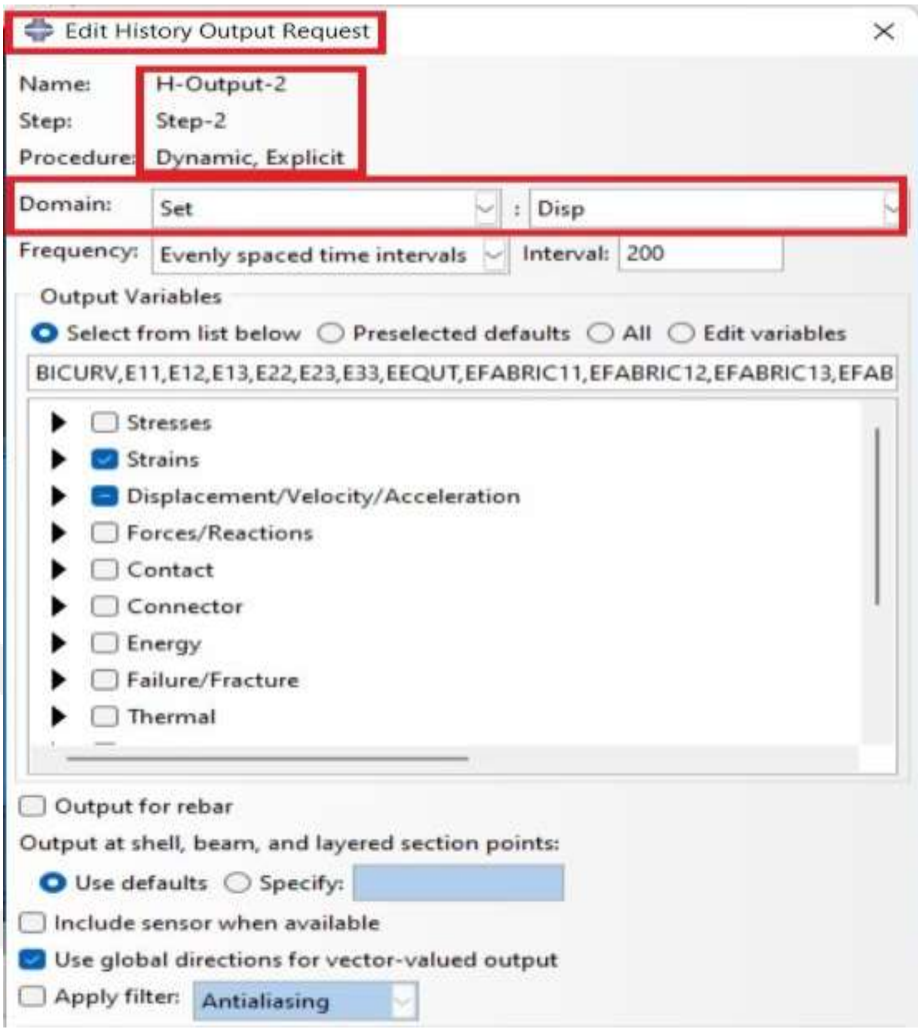

Figure 4.33 The outputting of displacement values

4.5 Results Discussion

The results of the simulation by ABAQUS software versus the results of the reference study in terms of force-displacement curves have been displayed in this part.

Regardless of the simplicity of the simulation procedure, the FE model curves have been presented with reasonably good agreement with both the experimental curves as well as ANSYS curves in the reference study for W, 2W2, and 1P1W1P1 specimens as in Figures 4.34, 4.35, and 4.36, respectively.

Therefore, the performance of the FE model in the current study by ABAQUS software has been capable of reproducing the observed behaviour except for the post-peak reduction of strength caused by the limitations of the parametric study to simulate stress-strain curves with negative slopes as mentioned in the reference study by (Karlos et al., 2020).

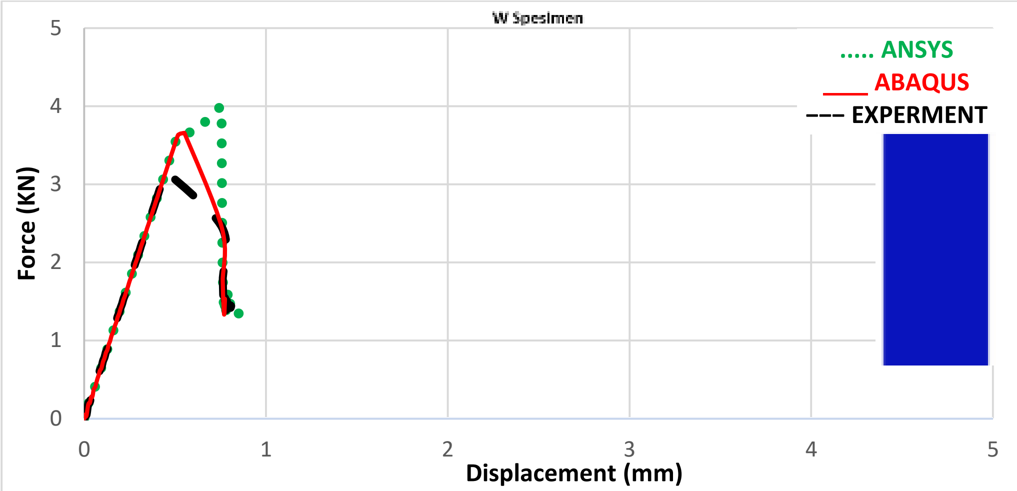

Figure 4.34 Force-displacement curves for control specimen

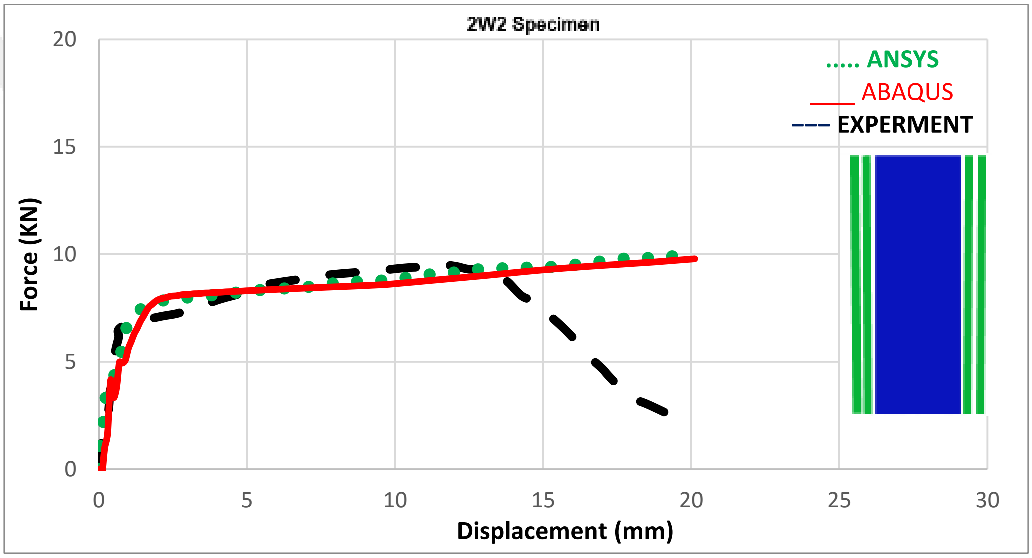

Figure 4.35 Force-displacement curves for 2W2 specimen

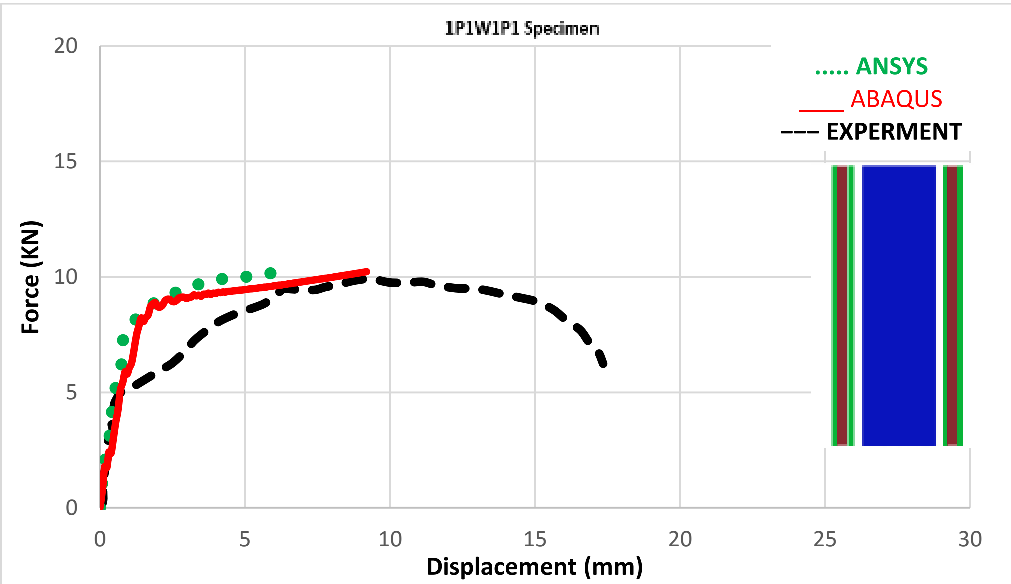

Figure 4.36 Force-displacement curves for 1P1W1P1 specimen

According to ABAQUS results, the control specimen (W) capacity is about 3.8 KN, as in Figure 4.34, and the capacity of the masonry wall is about 10 KN by implementing only TRM on both sides (2W2 specimen) as in Figure 4.35. Also, the capacity of the masonry wall is about 10 KN by combining the TRM with a TIP on both sides (1P1W1P1 specimen), as shown in Figure 4.36. The magnitude of displacement of the 2W2 and 1P1W1P1 specimens in the ABAQUS can be observed in Figures 4.37 and 4.38, respectively.

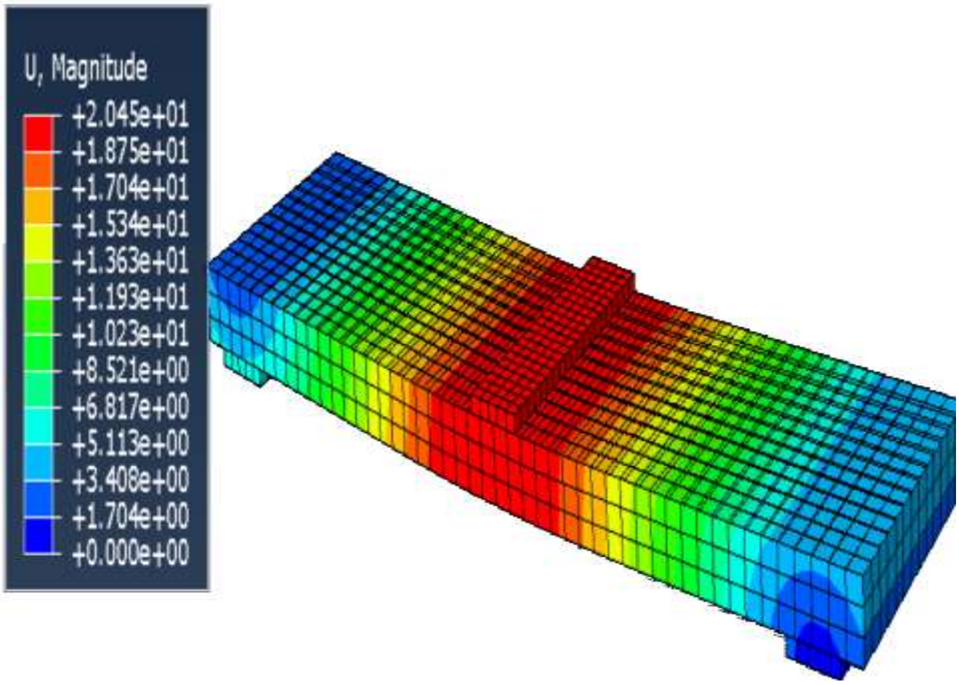

Figure 4.37 Displacement magnitude for 2W2 specimen by ABAQUS

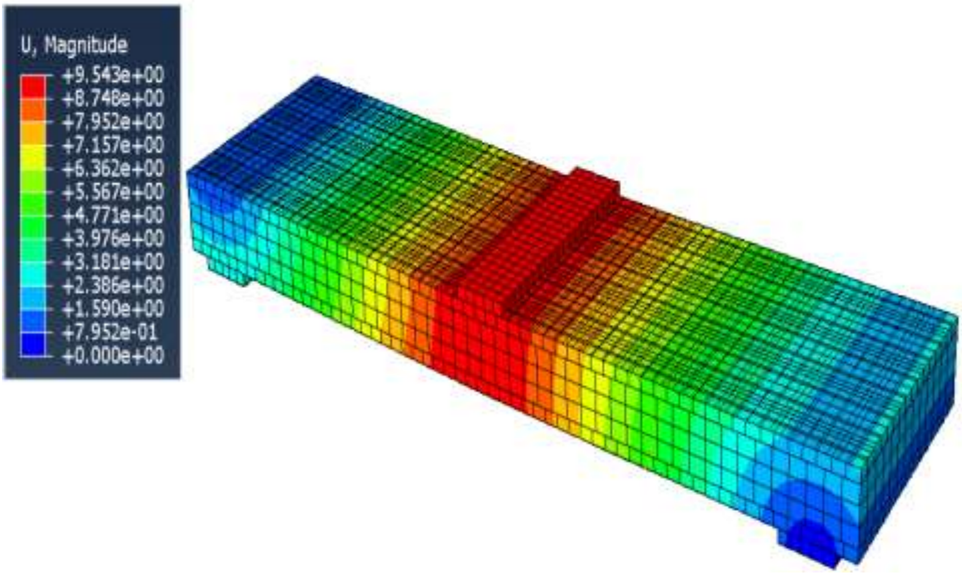

Figure 4.38 Displacement magnitude for 1P1W1P1 specimen by ABAQUS

Since the results of the FE approach agree with the reference study results, the TIP contribution without the TRM system (PWP specimen) and the contribution of TRM with TIP to one side of the wall (1P1W specimen) have been investigated in the current study where these two parameters have been not investigated in the reference study. The PWP specimen has been compared with the control specimen (W) to predict the TIP contribution without the TRM system for the masonry wall retrofitted as in Figure 4.39. The TIP contribution to the capacity of the masonry wall is about 4.9 KN, while the control specimen (W) capacity is about 3.8 KN. Therefore, the application of the TIP system without the TRM system increases the strength and deformation of the masonry wall capacity by a small percentage compared to the application of TIP with TRM as in the 1P1W1P1 specimen or the application of only TRM as in the 2W2 specimen. The magnitude of displacement of the PWP specimen is shown in Figure 4.40.

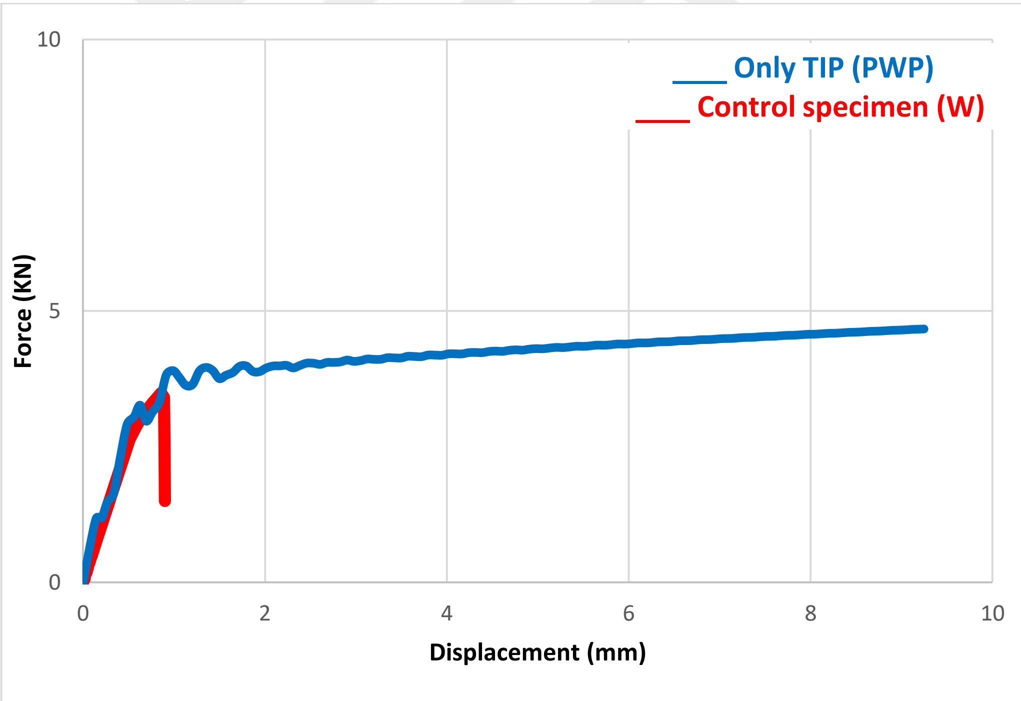

Figure 4.39 Force-displacement curves for PWP vs W

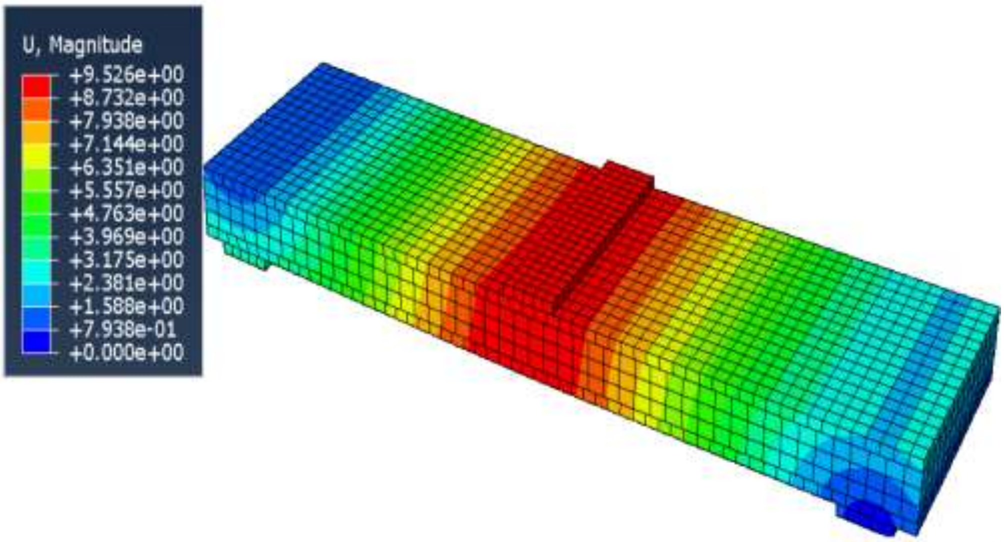

Figure 4.40 Displacement magnitude for PWP specimen by ABAQUS

The 1P1W specimen has been compared with the 1P1W1P1 specimen as in Figure 4.41 to assess the masonry wall capacity in the case of application of the TRM with TIP to one side of the wall. Based on Figure 4.41, the capacity of the masonry wall is about 5.2 KN in the case of retrofitting to one side (1P1W specimen). While the capacity of the masonry wall is about 10.2 KN in the case of retrofitting to both sides of the wall (1P1W1P1 specimen). Therefore, the masonry wall capacity in the case of retrofitting to one side is half the masonry wall capacity on both sides. The magnitude of displacement of the 1P1W specimen is displayed in Figure 4.42.

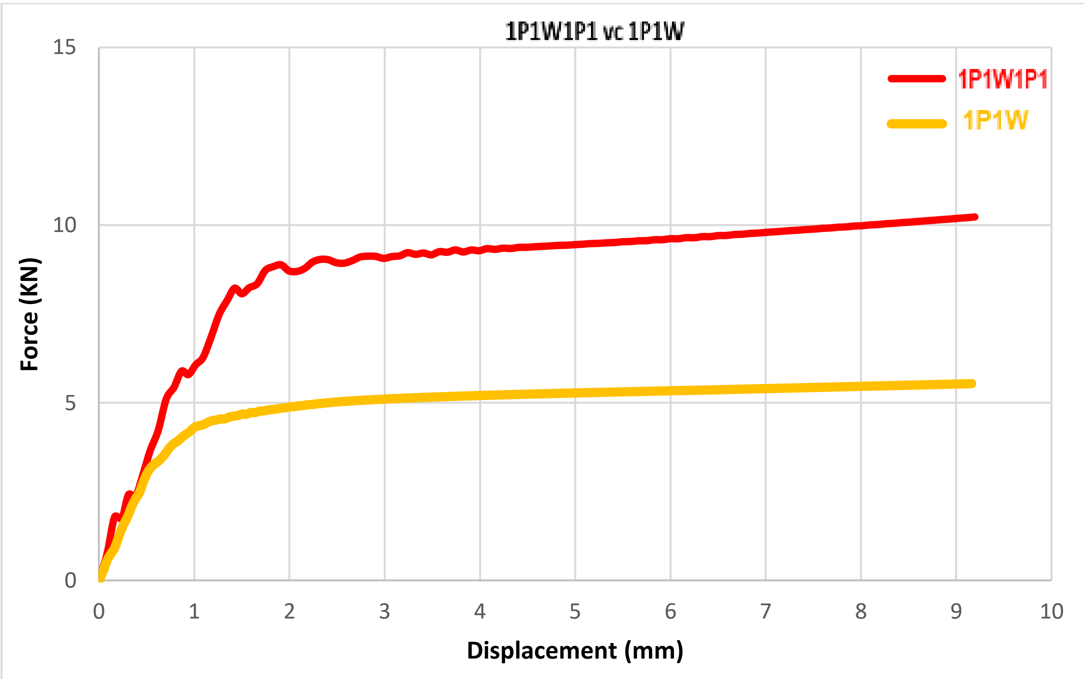

Figure 4.41 Force-displacement curves for 1P1W vs 1P1W1P1

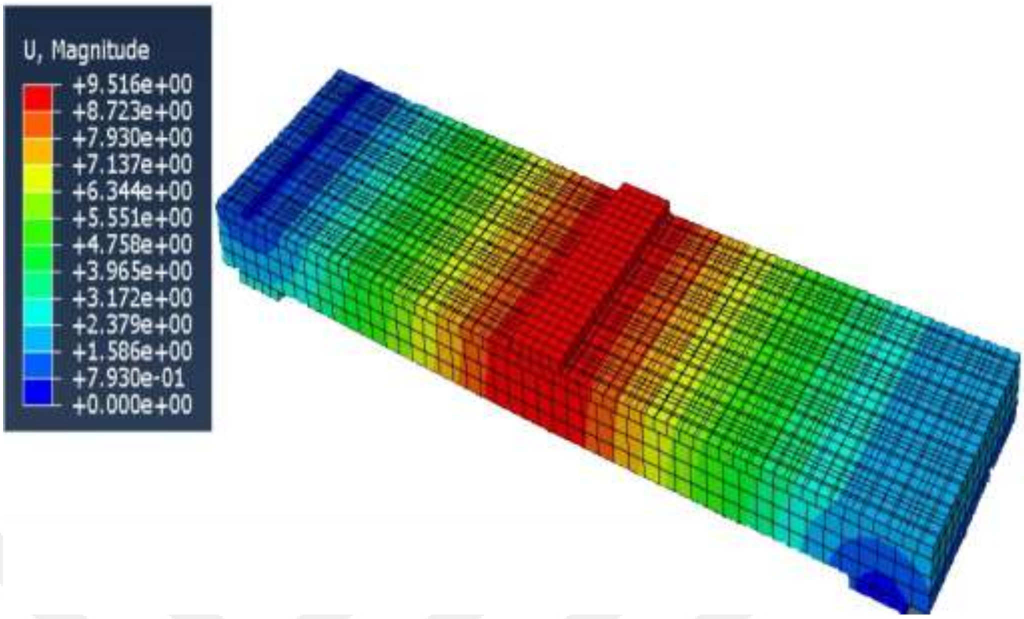

Figure 4.42 Displacement magnitude for 1P1W specimen by ABAQUS

Table 4.10 summarises the strength of masonry wall capacity by FE analysis with ABAQUS software for all specimens.

Table 4.10 The results of strength capacity for all specimens

Specimen	Masonry wall capacity
W	3.8 KN
2W2	10 KN
1P1W1P1	10 KN
PWP	4.8 KN
1P1W	5.5 KN

5. RESULTS, CONCLUSION, AND FUTURE WORK

This thesis contains two studies; the first study aims to access a precise theoretical approach for determining the capacity of TRM-reinforced masonry walls exposed to out-of-plane loading by various equations. A comparison of the results of these equations with the experimental database, which contains 108 URM walls retrofitted using TRM techniques and underwent out-of-plane loading, has been done. The prediction performance of the equations has been evaluated based on some statistical analysis by calculating the ratio between the experimental and theoretical ultimate moment for 64 specimens.

In contrast, the second study aims to develop a finite element (FE) method to simulate seismic and energy retrofitting for URM walls by TRM (textile-reinforced mortar) with TIP (thermal insulation panel) in the ABAQUS software. Five parameters have been investigated through FE analysis: unreinforced masonry wall as control specimen (W), only TRM composite has been bonded to both sides of the wall without TIP system (2W2), both the TRM system and TIP system have been bonded to both sides of the wall (1P1W1P1), only TIP system has been implemented to both sides of the wall without TRM systems (PWP), and both of TRM system and TIP system have been applied to only one side of the wall (1P1W). The results of the FE method have been compared with experimental and numerical study results in the literature.

Analytical results generally indicate that using the bond and tensile test results to obtain TRM stress-strain behaviour leads to accurate predictions. Also, The results indicated that the approach developed in the literature to predict the capacity of FRP-retrofitted URM walls provides acceptable results to predict the capacity of TRM-retrofitted URM walls.

Regarding numerical results, the results of the FE model with ABAQUS software agree with the results of the experimental and numerical study in the literature, indicating that the current study's simulation method could reproduce the observed behaviour. Therefore, this approach could be adopted in future works to improve the proposed approach. Also, the results show that applying only TIP on both sides of the wall without the application of TRM material increases strength and deformation capacity for masonry wall by a smaller percentage (about 50%) than the implementation of the TRM and TIP to both sides.

Finally, for future works, developing theoretical studies to assess the contribution of TRM with TIP to the retrofitted URM walls by using mechanics theories.

In addition, developing parametric studies to simulate the behaviour of retrofitted masonry to generalise the FE model and to know the effect of other parameters on the capacity of masonry walls, such as masonry types, masonry wall dimensions, TRM thickness, textile types, layers number of TRM, types of thermal material, and the positions of retrofitting materials.

REFERENCES

Abdulla, K. F., Cunningham, L. S., & Gillie, M. (2017). Simulating masonry wall behaviour using a simplified micro-model approach. Engineering Structures, 151, 349-365.

AC434. Acceptance criteria for masonry and concrete strengthening using fiberreinforced cementitious matrix (FRCM) composite systems. ICC-Evaluation Service, Whittier, CA; 2013.

ACI Committee 549, ACI 549.4R-13 – Guide to Design and construction of externally bonded fabric-reinforced cementitious matrix (FRCM) systems for repair and strengthening concrete and masonry structures, (2013)

Alecci, V., De Stefano, M., Luciano, R., Rovero, L., & Stipo, G. (2016). Experimental investigation on bond behavior of cement-matrix–based composites for strengthening of masonry structures. Journal of Composites for Construction, 20(1), 04015041

Anastaselos, D., Giama, E., & Papadopoulos, A. M. (2009). An assessment tool for the energy, economic and environmental evaluation of thermal insulation solutions. Energy and Buildings, 41(11), 1165-1171.

Arboleda D, Carozzi FG, Nanni A, Poggi C. Testing procedure for the uniaxial tensile characterization of fabric-reinforced cementitious matrix composites. J Compos Constr 2015. http://dx.doi.org/10.1061/(ASCE)CC.1943-5614.0000626.

Ascione L, de Felice G, De Santis S. A qualification method for externally bonded Fibre Reinforced Cementitious Matrix (FRCM) strengthening systems. Compos Part B Eng 2015;78:497-506.

Askouni, P. D., and Papanicolaou, C. G. (2016). Experimental investigation of bond between TRM overlays and masonry. In Structural Analysis of Historical Constructions: Anamnesis, Diagnosis, Therapy, Controls (pp. 315-322). CRC Press.

Babaeidarabad, S. (2013). Masonry walls strengthened with fabric-reinforced cementitious matrix composite subjected to in-plane and out-of-plane load. University of Miami.

Babaeidarabad, S., De Caso, F., & Nanni, A. (2014). URM walls strengthened with fabric-reinforced cementitious matrix composite subjected to diagonal compression. Journal of Composites for Construction, 18(2), 04013045

Bajpai, K., & Duthinh, D. (2003). Flexural strengthening of masonry walls with external composite bars. Mason Soc J, 21, 69-80.

Bedirhanoglu, I. (2015). Prefabricated-HSPRCC panels for retrofitting of existing RC members-a pioneering study. Structural engineering and mechanics: An international journal, 56(1), 1-25.

Bedirhanoglu, I., and Ilki, A. (2018, November). Fiber reinforced cementitious composites for retrofit of reinforced concrete members-A Review. In International Workshop on Advanced Materials and Innovative Systems in Structural Engineering: Seismic Practices (p. 122)

Bedirhanoglu, I., Ilki, A., and Triantafillou, T. C. (2022). Seismic Behavior of Repaired and Externally FRP-Jacketed Short Columns Built with Extremely Low-Strength Concrete. Journal of Composites for Construction, 26(1), 04021068.

Bedirhanoglu, I., Ilki, A., & Kumbasar, N. (2013). Precast fiber reinforced cementitious composites for seismic retrofit of deficient RC joints–a pilot study. Engineering Structures, 52, 192-206.

Bedirhanoglu, I., Ilki, A., & Triantafillou, T. (2019, December). Effect of pre-damage on the seismic behaviour of FRP retrofitted sub-standard short columns. In 7th Asia-Pacific Conference on FRP in Structures, APFIS 2019. APFIS Conference Series.

Belleri, A. and Marini, A. (2015), Does seismic risk affect the environmental impact of existing buildings?, Energy and Buildings, doi:10.1016/j.enbuild.2015.10.048

Bellini, A., Incerti, A., and Mazzotti, C. (2017). Out-of-plane strengthening of masonry walls with FRCM composite materials. In Key engineering materials (Vol. 747, pp. 158-165). Trans Tech Publications Ltd.

Bellini, A., Incerti, A., Bovo, M., and Mazzotti, C. (2018). Effectiveness of FRCM reinforcement applied to masonry walls subject to axial force and out-of-plane loads evaluated by experimental and numerical studies. International Journal of Architectural Heritage, 12(3), 376-394.

Benzar, B. E., Park, M., Lee, H. S., Yoon, I., and Cho, J. (2020). Determining retrofit technologies for building energy performance. Journal of Asian Architecture and Building Engineering, 19(4), 367-383.

Bernat-Maso, E., Escrig, C., Aranha, C. A., and Gil, L. (2014). Experimental assessment of Textile Reinforced Sprayed Mortar strengthening system for brickwork wallettes. Construction and Building Materials, 50, 226-236.

Boem, I. (2022). Masonry Elements Strengthened with TRM: A Review of Experimental, Design and Numerical Methods. Buildings, 12(9), 1307

Bomberg, M., Lstiburek, J., & Nabhan, F. (1997). Long-term, hygrothermal performance of exterior insulation and finish systems (EIFS). Journal of Thermal Insulation and Building Envelopes, 20(3), 227-248

Bothara, J. K., and Hiçyılmaz, K. M. (2008). General observations of building behaviour during the 8th October 2005 Pakistan earthquake. Bulletin of the New Zealand society for earthquake engineering, 41(4), 209-233.

Bothara, J. K., Dhakal, R. P., and Mander, J. B. (2010). Seismic performance of an unreinforced masonry building: An experimental investigation. Earthquake Engineering and Structural Dynamics, 39(1), 45-68.

Bucchi, F., Arangio, S., & Bontempi, F. (2013, September). Seismic assessment of an historical masonry building using nonlinear static analysis. In Proceedings of the 14th International Conference on Civil, Structural and Environmental Engineering Computing, Sardinia, Italy (Vol. 36).

Carozzi FG, Bellini A, D'Antino T, de Felice G, Focacci F, Hojdys L, et al. Experimental investigation on tensile and shear bond properties of Carbon-FRCM composites applied on masonry substrates. Compos Part B Eng 2017;128:100-119.

Carozzi, F. G., Colombi, P., and Poggi, C. (2015). Fabric reinforced cementitious matrix (FRCM) systems for strengthening of masonry elements subjected to out-of-plane loads. In Advanced Composites in Construction (pp. 182-188). GBR.

D’Ambrisi, A., Feo, L., & Focacci, F. (2013). Experimental and analytical investigation on bond between Carbon-FRCM materials and masonry. Composites Part B: Engineering, 46, 15-20.

D’Antino T, Carloni C, Sneed LH, Pellegrino C. Matrix-fiber bond behavior in PBO FRCM composites: a fracture mechanics approach. Eng Frac Mech 2014;117:94-111.

D’Antino T, Carozzi FG, Colombi P, Poggi C. A new pull-out test to study the bond behavior of fiber reinforced cementitious composites. Key Eng Mater 2017;747:258-265.

D’Antino T, Papanicolaou C. Mechanical characterization of textile reinforced inorganic-matrix composites. Compos Part B Eng 2017; 127:78-91.

D’Antino T, Pellegrino C, Carloni C, Sneed LH, Giacomin G. Experimental analysis of the bond behavior of glass, carbon, and steel FRCM composites. Key Eng Mat 2015;624:371-378.

D’Antino T, Pisani MA. Evaluation of the effectiveness of current guidelines in determining the strength of RC beams retrofitted by means of NSM reinforcement. Compos Struct 2017;167:166-177.

D’Antino T, Triantafillou TC. Accuracy of design-orineted formulations for evaluating the flexural and shear capacities of FRP-strengthened RC beams. Struct Concr 2016;17:425-442.

D'Antino, T., Carozzi, F. G., Colombi, P., & Poggi, C. (2018). Out-of-plane maximum resisting bending moment of masonry walls strengthened with FRCM composites. Composite Structures, 202, 881-896.

D'Antino, T., Calabrese, A. S., Pisani, M. A., & Poggi, C. (2022). Design of FRCM Strengthened Masonry Walls Subjected to Out-of-Plane Loading According to CNR-DT 215: Discussion of the α Coefficient. In Key Engineering Materials (Vol. 916, pp. 289-296).

De Felice, G., De Santis, S., Garmendia, L., Ghiassi, B., Larrinaga, P., Lourenço, P. B., ... and Papanicolaou, C. G. (2014). Mortar-based systems for externally bonded strengthening of masonry. Materials and structures, 47(12), 2021-2037

De Santis D, Ceroni F, de Felice G, Fagone M, Ghiassi G, Kwiecien A, Lignola GP, Morganti M, Santantandrea M, Valluzzi MR, Viskovic A. Round robin test on tensile and bond behavior of steel reinforced grout systems. Compos Part B Eng 2017;127:100- 120.

De Santoli, L., Bellia, L., Corgnati, S. P., d'Ambrosio, F. R., Filippi, M., & Mazzarella, L. (2014). Energy efficiency in historic buildings. Guida AiCARR n. III. Milano: Editoriale Delfino.

Dong, Z., Deng, M., Zhang, Y., Zhang, C., and Ma, P. (2020). Out-of-plane strengthening of unreinforced masonry walls using textile reinforced mortar added short polyvinyl alcohol fibers. Construction and Building Materials, 260, 119910.

Faella, C., Martinelli, E., Nigro, E., and Paciello, S. (2004, August). Tuff masonry walls strengthened with a new kind of C-FRP sheet: Experimental tests and analysis. In Proceedings of the 13th World Conference on Earthquake Engineering, Vancouver, BC, Canada (pp.1-6).

FEMA, 306 – Evaluation of Earthquake Damaged Concrete and Masonry Wall Buildings: Basic Procedures Manual, FEMA, Washington, DC, 1998.

Garmendia, L., San-José, J. T., García, D., and Larrinaga, P. (2011). Rehabilitation of masonry arches with compatible advanced composite material. Construction and Building Materials, 25(12), 4374-4385.

Gattesco, N., and Boem, I. (2017). Out-of-plane behavior of reinforced masonry walls: Experimental and numerical study. Composites Part B: Engineering, 128, 39-52.

Gkournelos, D. P., Bournas, D. A., & Triantafillou, T. C. Combined seismic and energy upgrading of existing buildings using advanced materials, EUR 29172 EN, Publications Office of the European Union, Luxembourg, 2019. doi, 10, 17376.

Gkournelos, P. D., Azdejković, L. D., and Triantafillou, T. C. (2022). Innovative and Eco-friendly Solutions for the Seismic Retrofitting of Natural Stone Masonry Walls with Textile Reinforced Mortar: In-and Out-of-Plane Behavior. Journal of Composites for Construction, 26(1), 04021061.

Hamoush, S. A., McGinley, M. W., Mlakar, P., Scott, D., and Murray, K. (2001). "Out of-plane strengthening of masonry walls with reinforced composites." J. Compos. Constr., 10.1061/(ASCE)1090-0268(2001) 5:3(139), 139–145.

Harajli, M., ElKhatib, H., and San-Jose, J. T. (2010). Static and cyclic out-of-plane response of masonry walls strengthened using textile-mortar system. Journal of materials in civil engineering, 22(11), 1171-1180.

Kariou, F. A., Triantafyllou, S. P., Bournas, D. A., and Koutas, L. N. (2018). Out-of-plane response of masonry walls strengthened using textile-mortar system. Construction and Building Materials, 165, 769-781.

Karlos, K., Tsantilis, A., and Triantafillou, T. (2020). Integrated Seismic and Energy Retrofitting System for Masonry Walls Using Textile-Reinforced Mortars Combined with Thermal Insulation: Experimental, Analytical, and Numerical Study. Journal of Composites Science, 4(4), 189.

Korkmaz, M., Ozdemir, M. A., Kavali, E., and Cakir, F. (2018). Performance-based assessment of multi-story unreinforced masonry buildings: The case of historical Khatib School in Erzurum, Turkey. Engineering Failure Analysis, 94, 195-213.

Koutas, L., Bousias, S. N., and Triantafillou, T. C. (2015). Seismic strengthening of masonry-infilled RC frames with TRM: Experimental study. Journal of Composites for Construction, 19(2), 04014048.

Koutas, L., Triantafillou, T. C., and Bousias, S. N. (2015). Analytical modeling of masonry-infilled RC frames retrofitted with textile-reinforced mortar. Journal of Composites for Construction, 19(5), 04014082.

Krevaikas.T Strengthening of unreinforced masonry structures with advanced composites, Ph.D. Dissertation, Dept. of Civil Engineering, University of Patras, Greece, 2005 (in Greek).

Le Chi, H., Louda, P., Le Van, S., Volesky, L., Kovacic, V., and Bakalova, T. (2019). Composite performance evaluation of basalt textile-reinforced geopolymer mortar. Fibers, 7(7), 63.

Lignola GP, Caggegi C, Ceroni F, De Santis S, Krajewski P, Lourenco PB, Morganti M, Papanicolaou C, Pellegrino C, Prota A, Zuccarino L. Performance assessment of basalt FRCM for retrofit applications on masonry. Compos Part B Eng 2017;128:1-18.

Longo, F., Cascardi, A., Lassandro, P., and Aiello, M. A. (2020). A new Fabric Reinforced Geopolymer Mortar (FRGM) with mechanical and energy benefits. Fibers, 8(8), 49.

Longo, F., Cascardi, A., Lassandro, P., and Aiello, M. A. (2021). Thermal and seismic capacity improvements for masonry building heritage: a unified retrofitting system. Sustainability, 13(3), 1111.

Magenes G., Calvi G.M., "In-plane seismic response of brick masonry walls", Earthquake Engineering & Structural Dynamics, 26 (11), 1091–1112, 1997.

Majumder, A., Stochino, F., Fernando, F., and Enzo, M. (2021). Seismic and Thermal Retrofitting of Masonry Buildings with Fiber Reinforced Composite Systems: A State of the Art Review.

Mazzucca S, Hadad HA, Kourdou I, Ombres L, Nanni A. Characterization of new composite materials for masonry rehabilitation. Key Eng Mater 2017;747:398-405.

Mazzucco G, D'Antino T, Salomoni V, Pellegrino C. Three-dimensional finite element modeling of inorganic-matrix composite materials using a mesoscale approach. Comp Part B Eng 2018.

http://dx.doi.org/10.1016/j.compositesb.2017.12.057

Mechtcherine, V., Schneider, K., and Brameshuber, W. (2016). Mineral-based matrices for textile-reinforced concrete. In Textile fiber composites in civil engineering (pp. 25-43). Woodhead Publishing.

Meriggi, P., G. de Felice, and S. De Santis. 2020. "Design of the out-of-plane strengthening of masonry walls with fabric reinforced cementitious matrix composites." Constr. Build. Mater. 240: 117946. https://doi.org/10.1016/j.conbuildmat.2019.117946

Mosallam, A. S. 2007. "Out-of-plane flexural behavior of unreinforced red brick walls strengthened with FRP composites." Composites, Part B 38 (5–6): 559–574. https://doi.org/10.1016/j.compositesb.2006.07.019

Mustafaraj, E., Yardim, Y., Corradi, M., & Borri, A.(2020). Polypropylene as a Retrofitting Material for Shear Walls. Materials, 13(11), 2503.https://doi.org/10.3390/ma13112503.

National Research Council, Guide for the design and construction of externally bonded fibre reinforced inorganic matrix systems for strengthening existing structures. CNR-DT 215/2018, CNR, Rome, Italy, 2018.

Padalu, P. K. V. R., Singh, Y., and Das, S. (2018). Efficacy of basalt fibre reinforced cement mortar composite for out-of-plane strengthening of unreinforced masonry. Construction and Building Materials, 191, 1172-1190.

Padalu, P. K. V. R., Y. Singh, and S. Das. 2019. "Out-of-plane flexural behaviour of masonry wallettes strengthened using FRP composites and externally bonded grids: Comparative study." Composites, Part B 176: 107302.

Papanicolaou, C. G., Triantafillou, T. C., Karlos, K., and Papathanasiou, M. (2007). Textile-reinforced mortar (TRM) versus FRP as strengthening material of URM walls: in- plane cyclic loading. Materials and structures, 40(10), 1081-1097

Papanicolaou, C. G., Triantafillou, T. C., Papathanasiou, M., and Karlos, K. (2008). Textile reinforced mortar (TRM) versus FRP as strengthening material of URM walls: out-of-plane cyclic loading. Materials and structures, 41(1), 143-157.

Parisi, F., Lignola, G. P., Augenti, N., Prota, A., & Manfredi, G. (2011). Nonlinear behavior of a masonry subassemblage before and after strengthening with inorganic matrix-grid composites. Journal of Composites for Construction, 15(5), 821

Prota, A., Marcari, G., Fabbrocino, G., Manfredi, G., and Aldea, C. (2006). Experimental in-plane behavior of tuff masonry strengthened with cementitious matrix–grid composites. Journal of Composites for Construction, 10(3), 223-233.

Sagar, S. L., Singhal, V., Rai, D. C., and Gudur, P. (2017). Diagonal shear and out-of-plane flexural strength of fabric-reinforced cementitious matrix–strengthened masonry walletes. Journal of Composites for Construction, 21(4), 04017016.

Shermi, C., and Dubey, R. N. (2017). Study on out-of-plane behaviour of unreinforced masonry strengthened with welded wire mesh and mortar. Construction and Building Materials, 143, 104-120.

Standard, B. (2005). Eurocode 6—Design of masonry structures—. British Standard Institution. London, (2005).

Tan, K. H., and M. K. H. Patoary. 2004. "Strengthening of masonry walls against out-of-plane loads using fiber-reinforced polymer reinforcement." J. Compos. Constr. 8 (1): 79–87. https://doi.org/10.1061 /(ASCE)1090-0268(2004)8:1(79).

Triantafillou, T. (2016). Strengthening of existing concrete structures: Concepts and structural behavior. In Textile fiber composites in civil engineering (pp. 303-322). Wood head Publishing.

Triantafillou, T. (Ed.). (2016). Textile fibre composites in civil engineering. Woodhead Publishing.Triantafillou, T. C. 1998. "Strengthening of masonry structures using epoxy-bonded FRP laminates." J. Compos. Constr. 2 (2): 96–104. https://doi.org/10.1061/(ASCE)1090-0268(1998)2:2(96)

Triantafillou, T. C. 1998. "Strengthening of masonry structures using epoxy-bonded FRP laminates." J. Compos. Constr. 2 (2): 96–104.

Triantafillou, T. C., & Papanicolaou, C. G. (2006). Shear strengthening of reinforced concrete members with textile reinforced mortar (TRM) jackets. Materials and structures, 39(1), 93-103.

Triantafillou, T. C., Karlos, K., Kapsalis, P., and Georgiou, L. (2018). Innovative structural and energy retrofitting system for masonry walls using textile reinforced mortars combined with thermal insulation: In-plane mechanical behavior. Journal of Composites for Construction, 22(5), 04018029.

Triantafillou, T. C., Karlos, K., Kefalou, K., and Argyropoulou, E. (2017). An innovative structural and energy retrofitting system for URM walls using textile reinforced mortars combined with thermal insulation: Mechanical and fire behavior. Construction and Building Materials, 133, 1-13.

Tripathy, D., Meghwal, P., and Singhal, V. (2020). Strengthening of lime mortar masonry wallettes using fiber-reinforced cementitious matrix. Journal of Composites for Construction, 24(6), 04020075.

Tumialan, J. G., N. Galati, and A. Nanni. 2003. "Field assessment of unreinforced masonry walls strengthened with fiber reinforced polymer laminates." J. Struct. Eng. 129 (8): 1047–1056.

Turco, V., Secondin, S., Morbin, A., Valluzzi, M. R., and Modena, C. (2006). Flexural and shear strengthening of un-reinforced masonry with FRP bars. Composites Science and Technology, 66(2), 289-296

Valdes, M., & Antonio, N. (2005). STRENGTHENING OF STONE MASONRY COLUMNS BY MEANS OF CEMENT-BASED COMPOSITE WRAPPING. In Composites in Constructions 2005–Third International Conference.

Valluzzi, M. R., Da Porto, F., Garbin, E., and Panizza, M. (2014). Out-of-plane behaviour of infill masonry panels strengthened with composite materials. Materials and structures, 47(12), 2131-2145.

Yön, B. (2021). Identification of failure mechanisms in existing unreinforced masonry buildings in rural areas after April 4, 2019 earthquake in Turkey.

Valluzzi, M. R., Da Porto, F., Garbin, E., and Panizza, M. (2014). Out-of-plane behaviour of infill masonry panels strengthened with composite materials. Materials and structures, 47(12), 2131-2145.

Yön, B. (2021). Identification of failure mechanisms in existing unreinforced masonry buildings in rural areas after April 4, 2019 earthquake in Turkey.

CURRICULUM VITAE

Personal Information

Surname, Name	HAMZA TAHAT
Web Page (Research Gate, Academia, etc.)	

Education

Degree	Institution	Year of Graduation
MS	NATURAL AND APPLIED SCIENCES OF DİCLE UNIVERSITY	2022
BS	Cyprus International University- CIVIL ENGINEERING/ Northern Cyprus	2020
High School	OMAR AL-LAFI/ AS-SAREEH- IRBID-JORDAN	2016

Foreign Languages

Arabic- English

DİCLE ÜNİVERSİTESİ
FEN BİLİMLERİ ENSTİTÜSÜ
TEZ BENZERLİK BİLDİRİMİ FORMU

Öğrencinin Adı, Soyadı	HAMZA TAHAT
Öğrenci No	20806037
Ana Bilim Dalı	İnşaat Mühendisliği
Program Türü	Proje ☐ Yüksek Lisans ☒ Doktora ☐
Tez Danışmanı (Ünvanı, Adı, Soyadı)	Doç. Dr. İdris BEDİRHANOĞU
(Varsa) II. Tez Danışmanı (Ünvanı, Adı, Soyadı)	
Tez Başlığı	**INVESTIGATING SEISMIC AND ENERGY RETROFITTING BY IMPLEMENTING INNOVATIVE MATERIALS AND TECHNIQUES FOR MASONRY BUILDINGS**
RAPOR BİLGİLERİ	
Raporlama Aşaması	Tez Savunma Sınavı Sonrası
Sayfa Sayısı	80
Raporlama Tarihi	30.07.2022
Benzerlik Oranı (%)	14%

Yukarıda bilgileri verilen tez çalışmamın toplam 80 sayfalık kısmına ilişkin, 30/07/2022 tarihinde şahsım/tez danışmanım tarafından *Turnitin* isimli intihal tespit programından aşağıda belirtilen filtrelemeler uygulanarak alınmış olan intihal raporuna göre, tezimin benzerlik oranı 14% olarak tespit edilmiştir.

Uygulanan filtrelemeler:
☒Başlangıç Bölümleri (Kabul ve Onay sayfası, Teşekkür sayfası, Özet/Abstract) hariç
☒Kaynaklar hariç
☒Alıntılar hariç/dâhil
☐Diğer (Her şey dahil)

Tezimin benzerlik oranı, Dicle Üniversitesi Fen Bilimleri Enstitüsü İntihal Raporu Uygulama Esaslarında belirtilen üst sınır benzerlik oranını aşmamaktadır. Benzerlik oranım üst sınır benzerlik oranının altında olsa dahi aksinin tespit edilmesi durumunda her türlü yasal sorumluğu kabul ettiğimi ve hukuki sonuçlarına razı olduğumu bildirir,
gereğini arz ederim.

Öğrencinin Adı, Soyadı: HAMZA TAHAT
Tarih:
İmza:

Danışman Adı, Soyadı: Doç. Dr. İdris BEDİRHANOĞLU   İmza:

Tarih:

Ana Bilim Dalı Başkanı: Adı, Soyadı: Prof. Dr. Z.Fuat TOPRAK   İmza:

Tarih: